Two Forms of Instability in Geotechnical Engineering

Jacqueline Leclair

A Thesis
in
The Faculty
of
Engineering

Presented in Partial Fulfillment of the Requirements
for the degree of Master of Engineering at
Concordia University
Montreal, Quebec, Canada

April 1983

ABSTRACT

TWO FORMS OF INSTABILITY IN GEOTECHNICAL ENGINEERING

Jacqueline Leclair

This thesis presents an attempt to analyse two distinct types of instability situations which may be encountered in Geotechnical Engineering.

The first situation is concerned with the flow of liquefied sand. For this purpose, a special flume was built and the experiments conducted. The sand was brought to a state of liquefaction through the application of an upward hydraulic gradient. From the tests performed, it was observed that the application of the Unsteady-boundary-layer Theory was possible and therefore proceeded to the treatment of the problem as such.

The second problem deals with a special mode of hydraulic fracturing of clays as reported experimentally by Lefebvre, Philibert, Bozozuk, and Pare (1981). The analysis uses the Mindlin formulation and the superposition principle. It is shown that fracturing is the result of the hydraulic forces exceeding the tensile strength of the clay which are indirectly related to the in-situ stresses.

ACKNOWLEDGEMENT

My sincere appreciation goes to my supervisor, Dr. H.B. Poorooshasb, without his cooperation, guidance and fruitful suggestions this thesis would not have existed.

Credit is also due to Mr. R. Lombardo for his technical assistance and helpful ideas; Mr. E. Heasman and Mr. O. Kowalewski for building the earthquake flume; and Mr. W. Cross for his help with the photographs included in this thesis. Their thoroughness and care are greatly appreciated.

The author is grateful to the National Science and Engineering Council of Canada for the financial assistance.

Finally, I owe a debt of gratitude to my family for their unfailing moral support. I can offer here only an inadequate acknowledgement of my appreciation.

TABLE OF CONTENTS

LIST OF SYMBOLS

b_n	Coefficients of series expansion
c	Celerity
C	Cohesion
e	Void ratio
E	Modulus of Elasticity
g	Acceleration due to gravity
G	Modulus of rigidity
G_s	Specific Gravity
h	Flow depth
h_r	Hydraulic radius
H_o	Dam height
I	Influence value
K_o	Coefficient of earth pressure at rest
L	Length
n	Manning's coefficient of roughness
P	Pressure, load
r	Radius of pipe or piezometer
R	Chezy's coefficient
S	Strength parameter
t	time
t_f	freezing time
u	Pore water pressure, displacement, velocity of flow in the horizontal direction
v	Velocity of flow in the vertical direction

w	Displacement
x	Horizontal distance
x_f	Inundation distance
y	Vertical distance
z	Position, vertical distance
γ	Total unit weight, engineering shear strain
$\dot{\gamma}$	Strain rate
η	Viscosity
λ_m	Coefficients
μ	Viscosity
μ_p	Plastic viscosity
ν	Kinematic viscosity of fluid, Poisson's ratio
ξ	Position of load
ρ	Density
σ	Normal stress
τ	Shear strength
τ_y	Yield shear strength
ϕ	Angle of internal friction
ψ	Stream function
Θ	Slope inclination angle

LIST OF FIGURES

LIST OF TABLES

TO THE MEMORY OF MY BELOVED GRANDFATHER

KLAUS KUHL

CHAPTER 1

INTRODUCTION

In this chapter, the practical implications of the instability of sand deposits due to liquefaction and those of the instability of clays due to hydraulic fracturing will be discussed. In addition, the scope and objectives of this thesis will be presented.

1.1 Background

1.1.1 Instability of sand deposits due to liquefaction

The mining industry is an important component of the Canadian economy. The principal waste material from the mining and milling operations in which the valuable minerals have been recovered is called "mine tailings". See Fig. 1.1 for a typical mine waste disposal system.

Tailings have a wide variation of grain size distribution, depending on mill operation, but usually range from coarse sand to colloidal material (Fig. 1.2). Because tailings have no commercial value, their disposal is often given little or no consideration.

There is one aspect of tailings deposits that involves public concern: that a failure of a dam in which large volumes of water and semi-fluid tailings are released may not only cause extensive downstream pollution but also pose a serious threat to life and property.

A characteristic common to most tailings dam failures is that mine tailings tend to liquefy and flow over substantial

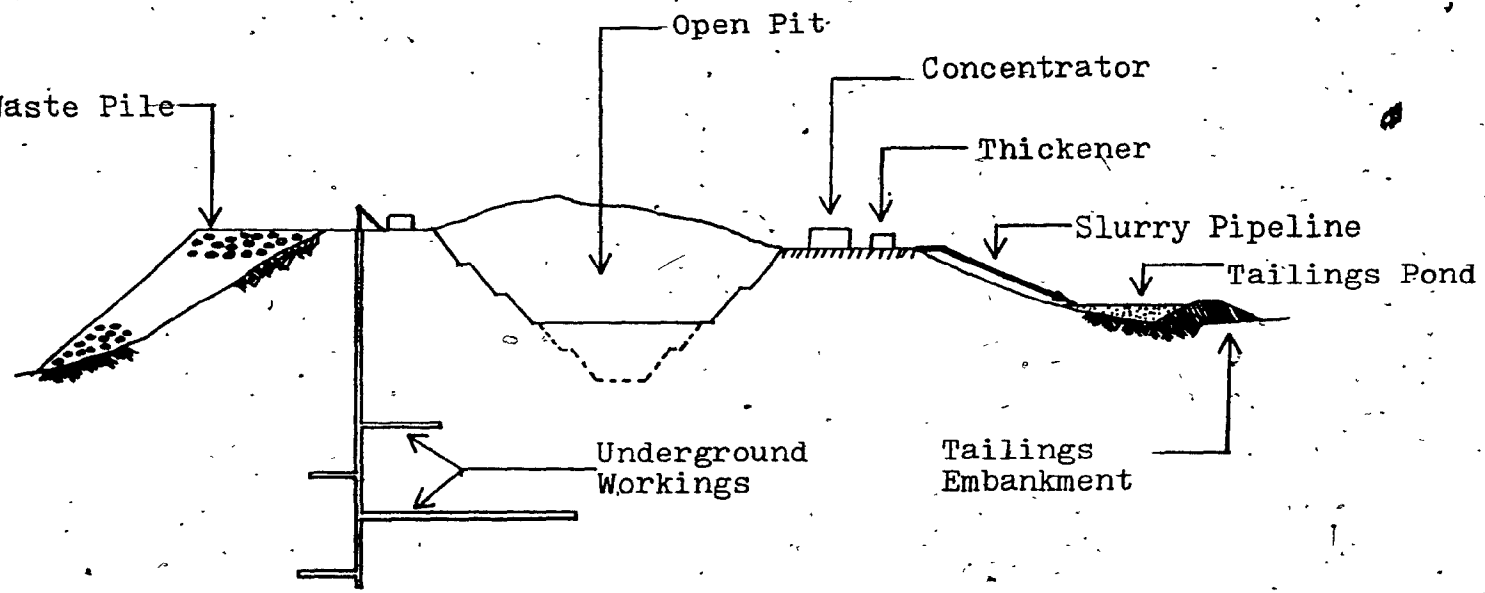

Fig. 1.1

Typical Mine Waste Disposal System

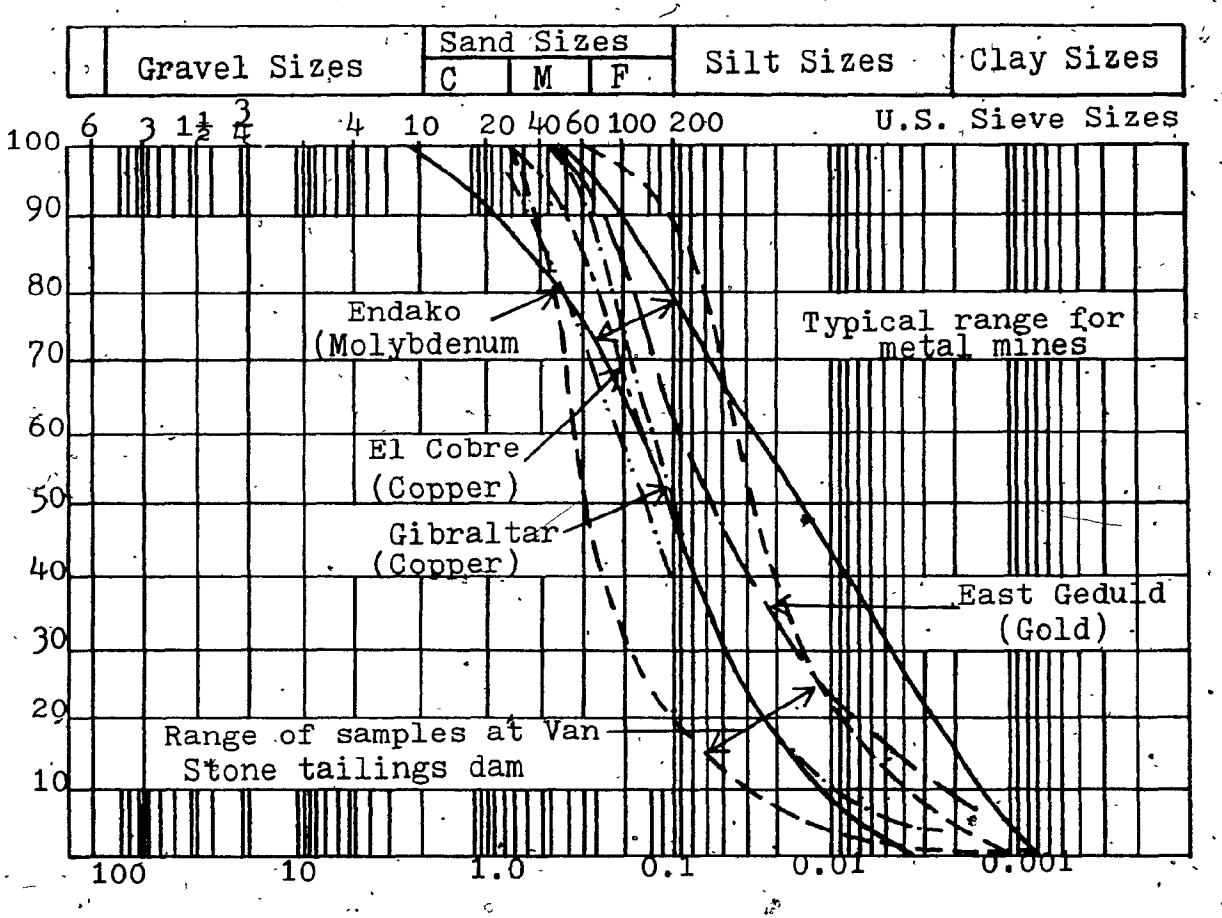

Fig. 1.2

Gradation of Typical Mine Tailings

distances. Failures of El Cobre Dam, Chile (1965), Aberfan, Wales (1966), Buffalo Creek, West Virginia (1972), Mochikoshi Dam, Japan (1978) are examples of such catastrophic dam incidents. In these 4 incidents, 450 lives were lost, and the loss of property was approximately $200 Million Jeyapalan (1980).

This thesis will analyse the behaviour of liquefied sand deposits as they are of great importance in assessing the potential for damage in case of a tailings dam failure.

1.1.2 Instability of clays due to hydraulic fracturing

Hydraulic fracturing: If liquid is pumped into a borehole to a sufficient pressure, the tangential stresses in the surface of the hole due to the external stresses and the pressure will become tensile, and extension fracture will occur if this stress exceeds the tensile strength of the material. A joint or fissure intersecting the hole which is held "closed" by the initial compressive stress field may be "opened" by tensile stresses when internal pressure is applied. For example, for a number of underground drill holes into Rand quartzite the holes would not accept water at pressures below 1.5 - 2.5 times the overburden pressure, but at some pressure in this range would suddenly take water quite freely.

The method is much used in the oil industry to increase yields. In this case a length of the hole is sealed off with packers at its ends so that pressure can be applied only to a restricted range of depths in the hole. Jeager and Cook (1979)

The use of hydraulic fracture in cohesive soils to determine lateral stresses in situ is relatively recent (Bjerrum et. al, 1972; Bjerrum and Andersen, 1972). The idea of using this method in soil mechanics was conceived by Bjerrum and Andersen while interpreting results from ordinary in-situ permeability tests in clay. It was then discovered that when establishing a water pressure higher than a certain critical value, the permeability apparently increased abruptly. The reason for this is that cracking occurs in the soil around the piezometer tip when the water pressure gets large enough to cause tensile stresses in the soil next to the piezometer, thus resulting in a sudden increase in flow of water into the soil.

Another instance where hydraulic fracturing of clays has been encountered is the fracturing of the core of an embankment dam. The formation of hydraulically induced cracks in the core can occur when the water pressure at a given depth exceeds the total stress of the core at the same depth, as will be described later in this thesis.

This thesis will present an analysis of this special mode of hydraulic fracturing based on the Mindlin formulation and the superposition principle.

1.2 Scope of the Work

The purpose of the research studies described in this thesis is to further the understanding of the behaviour of liquefied sand deposits during flow, and to provide an

analytical approach to the special mode of hydraulic fracturing of clays.

The study involves the following types of investigations:

a) Review of the available literature on the behaviour of liquefied tailings and similar earth materials.

b) Review of the Unsteady-boundary-layer Theory.

c) Review of the available literature on the stress-strain rate relationships of non-Newtonian fluids.

d) Experimental study of the flow of liquefied sand deposits.

e) Review of the literature on hydraulic fracturing.

f) Review of the Mindlin formulation.

g) Experimental study of hydraulic fracturing in clays.

1.3 Organization of the Thesis

The studies undertaken to achieve the objectives of this thesis are described in subsequent chapters.

Chapter 2, and 3 are devoted to the liquefaction problem. In Chapter 2 the apparatus, material, and test results are discussed and in Chapter 3 the results analysed.

Chapter 4, and 5 present a discussion of hydraulic fracturing tests performed and the analysis of these results respectively.

The thesis is concluded in Chapter 6 in which a summary of the main findings and recommendations for further research is presented.

CHAPTER 2

FLUME STUDIES ON LIQUEFIED SAND

2.1 Introduction

In this chapter, a series of flume studies on liquefied sand will be described. The details of the test material, the test apparatus as well as the description of the tests and results will be presented.

2.2 Test Material

The soil used in this work is a sand mixture with particle sizes ranging from silt size to medium-coarse sand. The sieve analysis shown on Fig. 2.1 illustrate a typical gradation curve of the mixture used in this research. Some properties of the sand are given in Table 2.1 shown below.

Table 2.1

Material Properties

Material	Property	Numerical Value
Sand Mixture	Cohesion	C = 0
"	Maximum void ratio	$e_{max} = 0.87$
"	Minimum void ratio	$e_{min} = 0.62$
"	Specific Gravity	$G_s = 2.65$
"	Angle of Shearing Resistance	$\phi = 32^{\circ}$

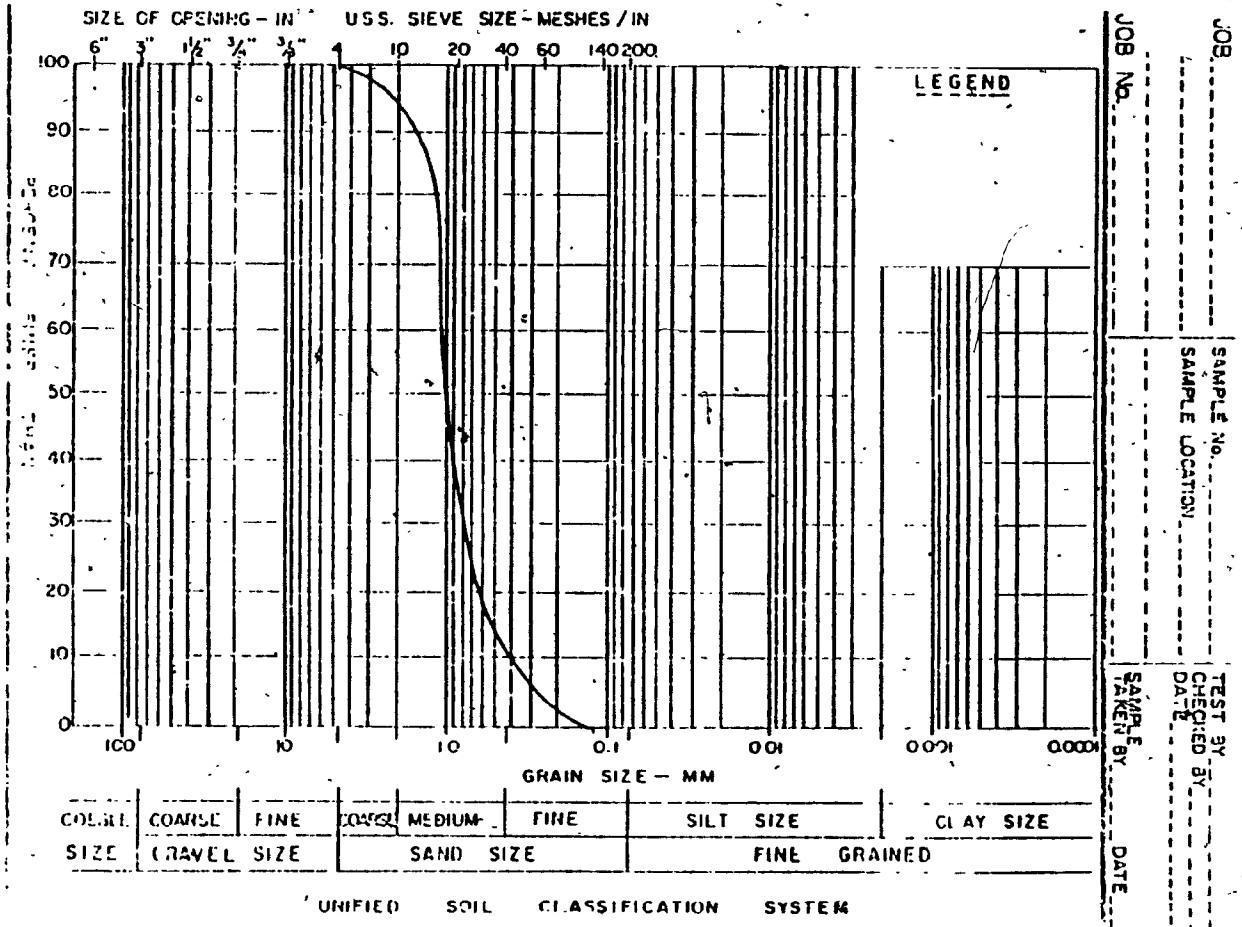

Fig. 2.1

Sieve Analysis

2.3 Test Apparatus

The experiments on liquefaction of sands were performed on a 1 foot wide, 8 foot long, plexiglass walled flume which was built especially for this research project. See Fig. 2.2

The bottom of the flume consists of a 8 foot long, 1 foot wide, 4 inch high, 5/8 inch thick aluminum channel. The sides of the flume consist of 2 plexiglass sheets 3/4 inch in thickness, 8 feet-4 inches in length, and 2 feet-3/4 in. in height which run longitudinally; and 2 aluminum plates 1 foot wide, 2 feet-3/4 in. high and 5/8 in. thick which run transversally.

The hydraulic system is composed of 2 lines of tap water carried by two 3/4 in. inside diameter copper pipes which before merging into one $1\frac{1}{4}$ in. copper pipe have their independent valves to control the flow as required in the experiment. The $1\frac{1}{4}$ in. inside diameter copper pipe finishes into a distribution box made of aluminum sheeting with dimensions: 8 in. x $5\frac{1}{2}$ in. x $1\frac{3}{4}$ in.. The purpose of this box is to eliminate to some degree the turbulence of the water entering the system. Out of the box run 3 copper pipes $1\frac{1}{4}$ in. inside diameter which extend over a distance of 4 feet. Along their length, these 3 pipes have 280 holes (1/8 in. in diameter) increasing in spacing as the distance from the source increases to make up for the head loss across the length of the pipes.

On top of these 3 pipes lies a stainless steel screen with dimensions: 11 in. x 48 in.. The function of this screen is to obtain a pressure distribution across the longitudinal area as uniform as possible. Four inches above this screen

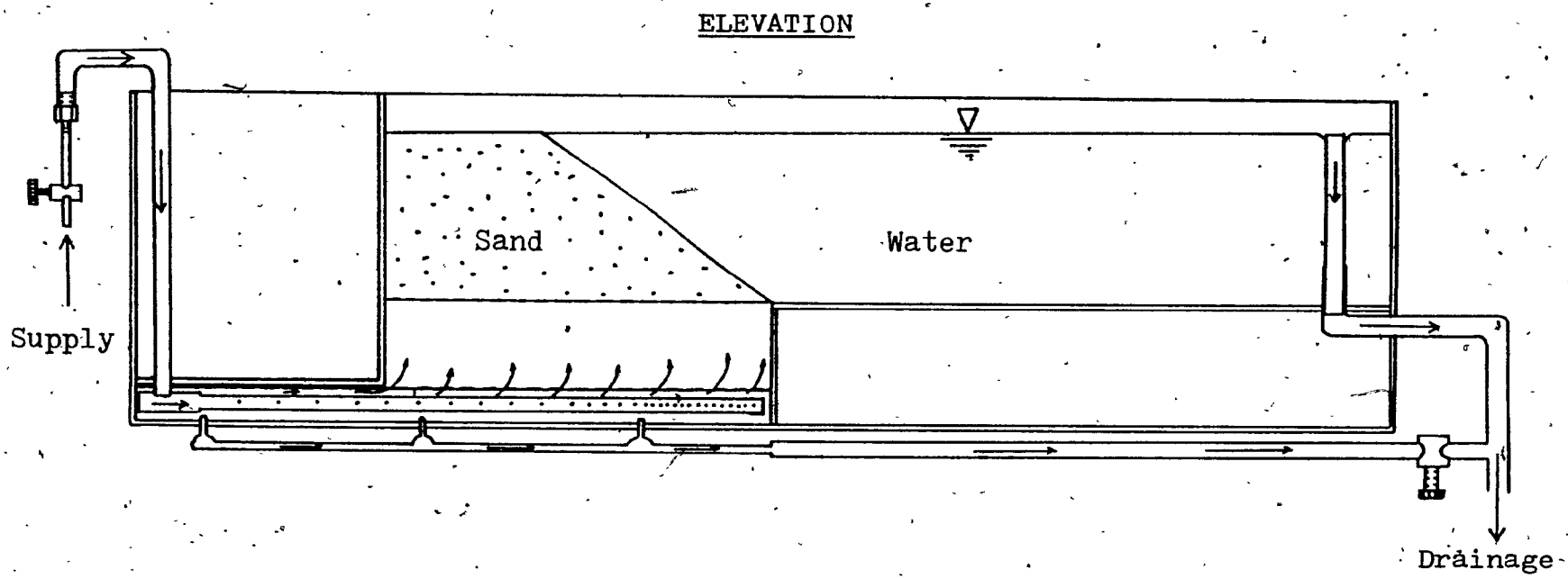

Fig. 2.2

Liquefaction Flume

lies a stainless steel mesh which supports the sand deposit, this allows an even distribution of pressure across the sand bed.

The drainage system consists of an elbow 1½ in. in diameter with a 1¼ in. inside diameter copper pipe which is adjustable in height. This piece allows the water level to be maintained at the desired height.

2.4 Description of Tests

The tests were always performed following the sequence described below.

a) The flume is filled with water.

b) A bed of sand is deposited under water through a funnel from a prescribed height to ensure the deposition of the sand in the loosest condition. The total height of the bed of sand varies from one test to another, but in general it is in the range of 8 to 13 inches.

The slope angle of the sand deposit is also varied from test to test; however, the maximum angle is always prescribed by the angle of repose of the sand used.

c) Water is allowed to flow across the sand bed with the aid of one of the valves described above. Then, the sand is brought to a state of liquefaction through a sudden application of an upward hydraulic gradient applied with the aid of the second valve. As the pore water pressure tends to levels comparable or equal to the normal stress, σ, then according to equation 2.1, the soil loses its strength and flows like

a viscous fluid.

$$\tau = (\sigma - u) \sin\phi \qquad \text{Eq. 2.1}$$

$$\tau \rightarrow 0$$

$$(\sigma - u) \sin\phi \rightarrow 0$$

$$u \rightarrow \sigma$$

Thus, simulating the instability caused by an earthquake.

d) The liquefied sand movement is photographed using a 35 mm. Nikon Camera.

e) The series of tests are performed varying the initial slope of the sand deposit, the height of the bed, and in some instances the gradation of the sand.

2.5 Test Results

Some typical results are shown in Fig 2.3 through Fig. 2.8.

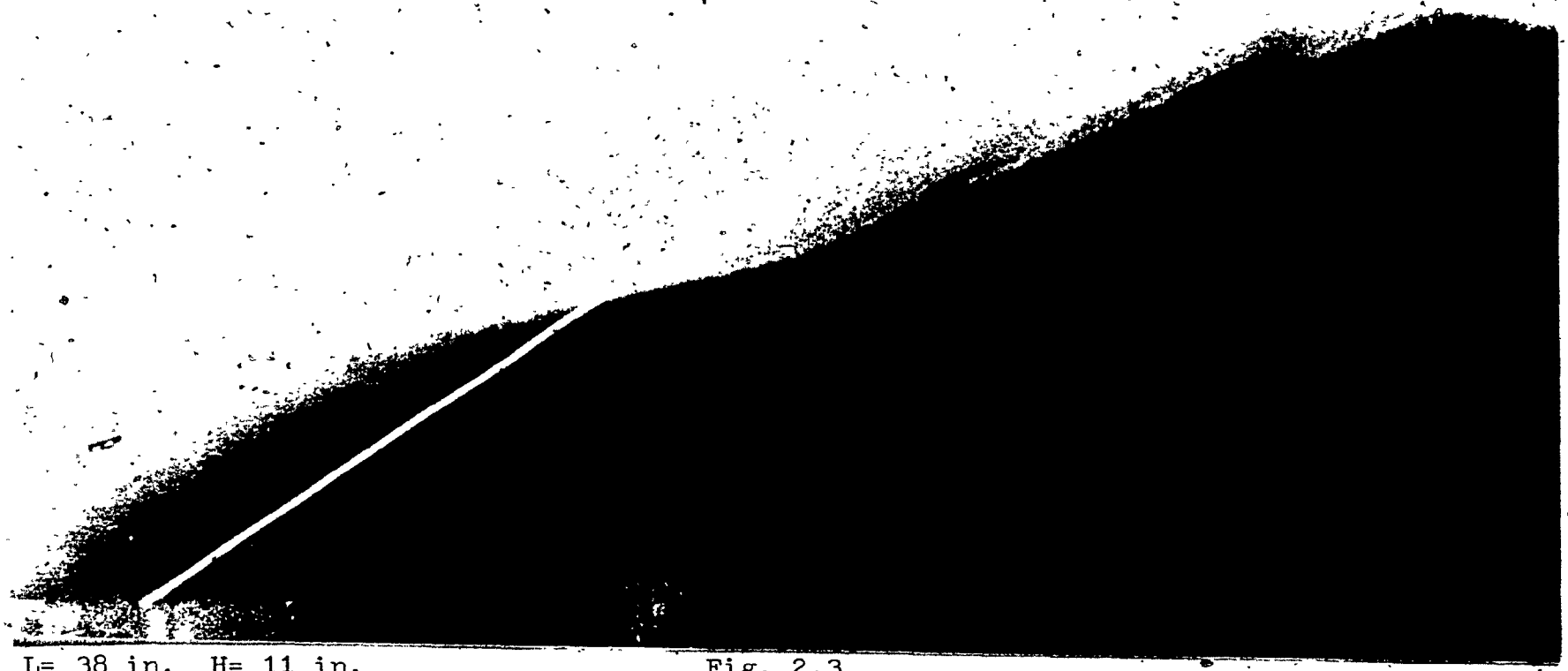

L= 38 in. H= 11 in.
Θ= 33.5° No Step
Uniform Coarse Sand

Fig. 2.3

Liquefaction Test 1

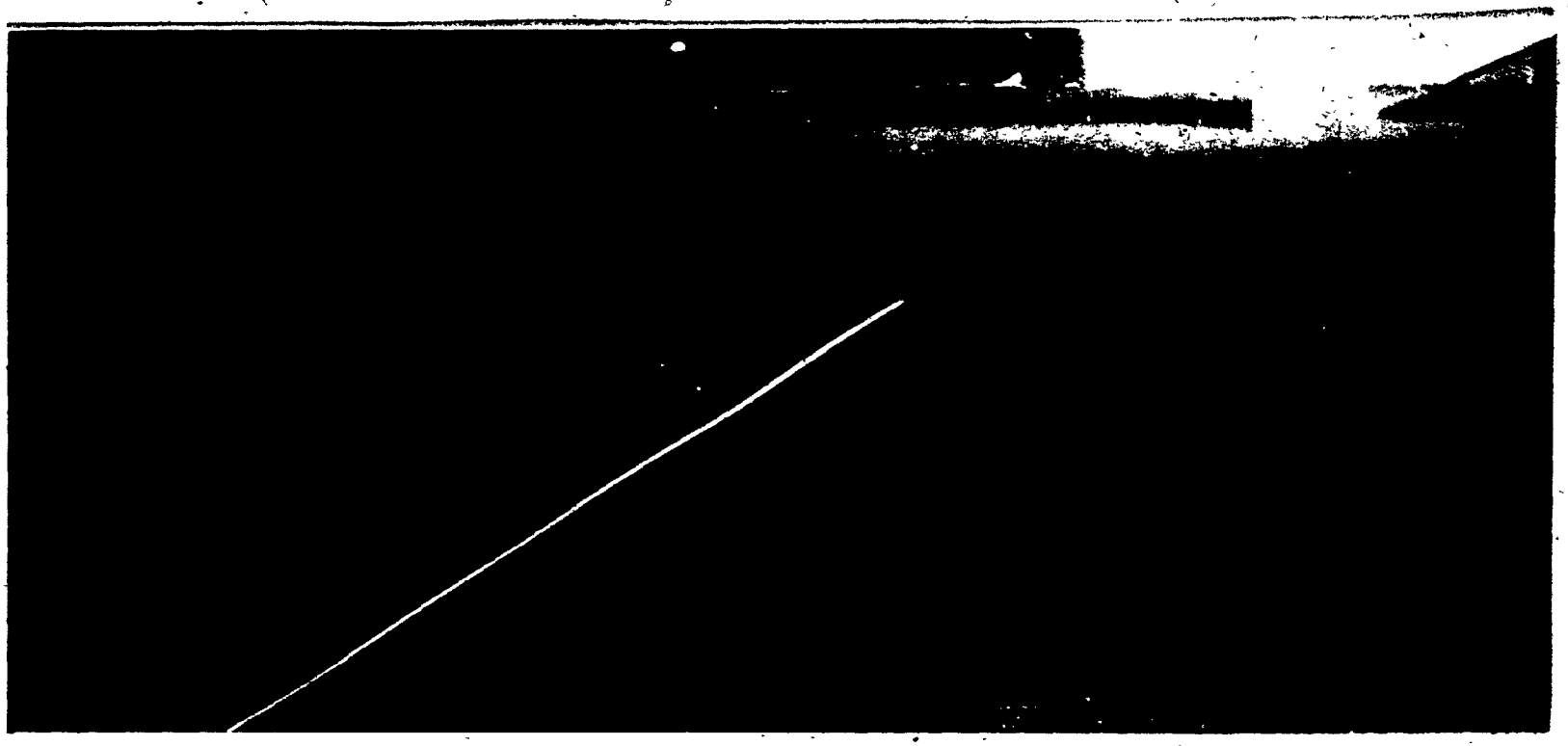

L = 35 in. H = 12 in.
Θ = 33° No step
Sand Mixture

Fig. 2.4

Liquefaction Test 2

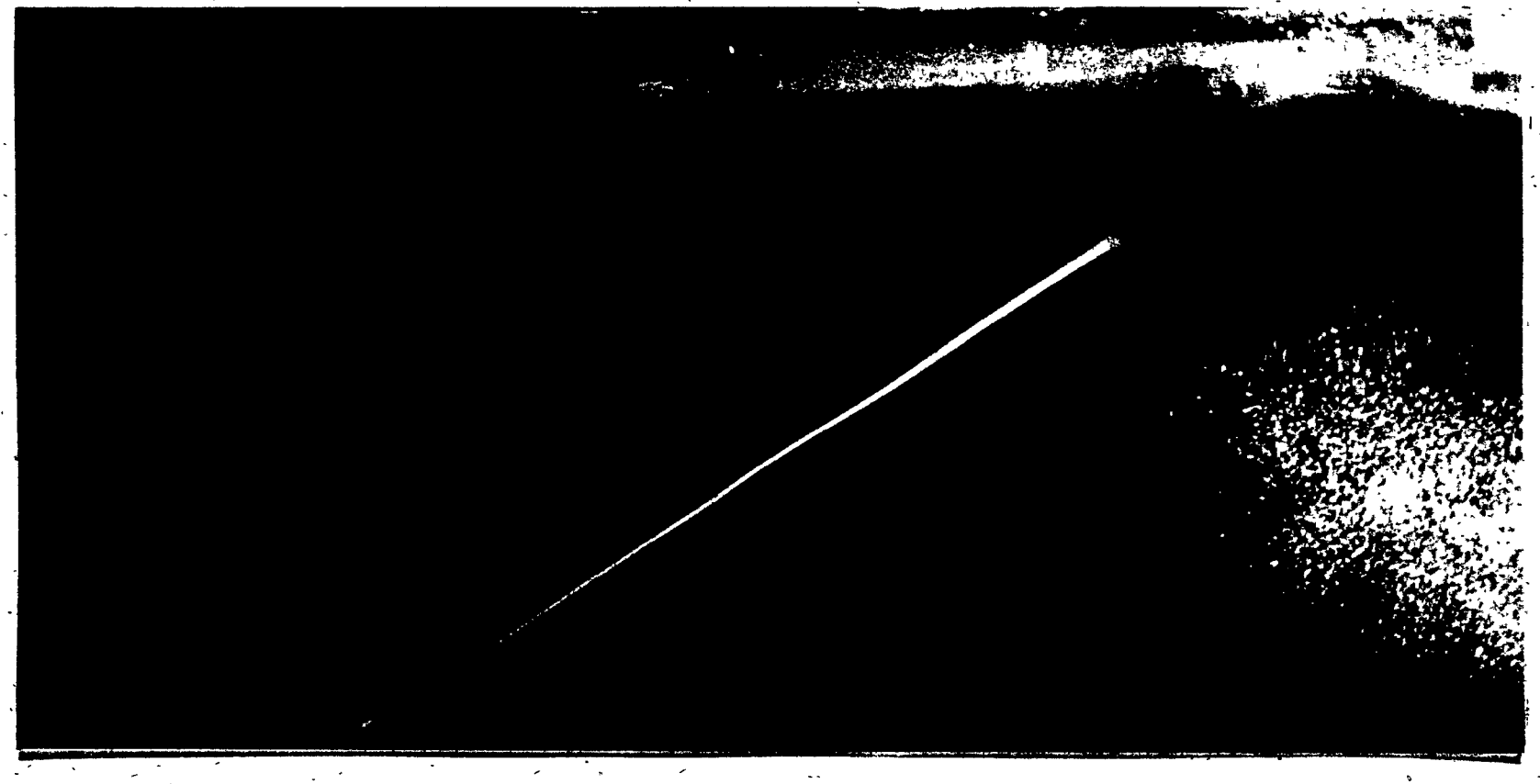

L = 51 in. H = 12 in.
θ = 32.5° No Step
Uniform Coarse Sand

Fig. 2.5

Liquefaction Test 3

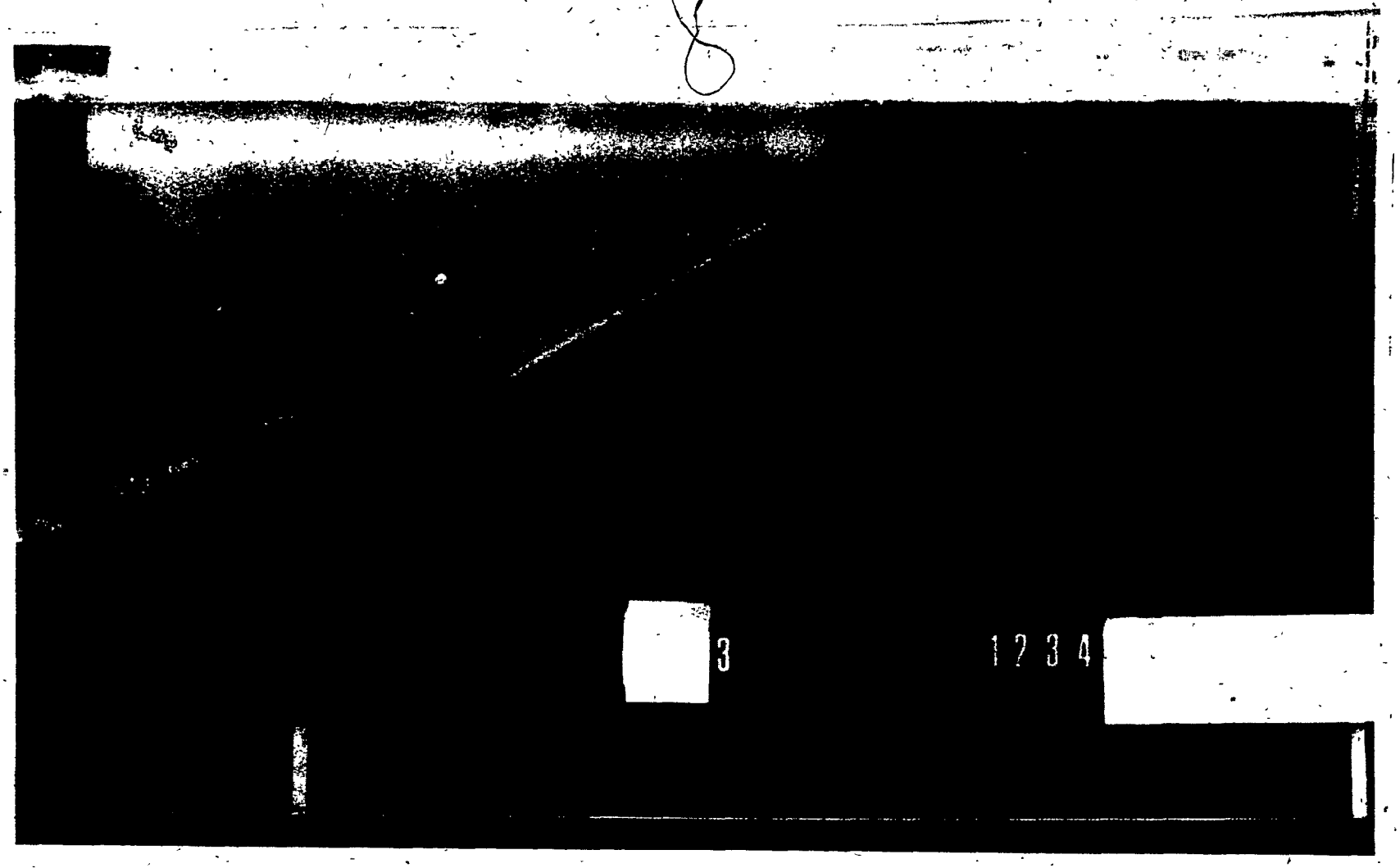

L = 31 in. H = 14 in.
θ = 31.5° With Step
Sand Mixture

Fig. 2.6

Liquefaction Test 4

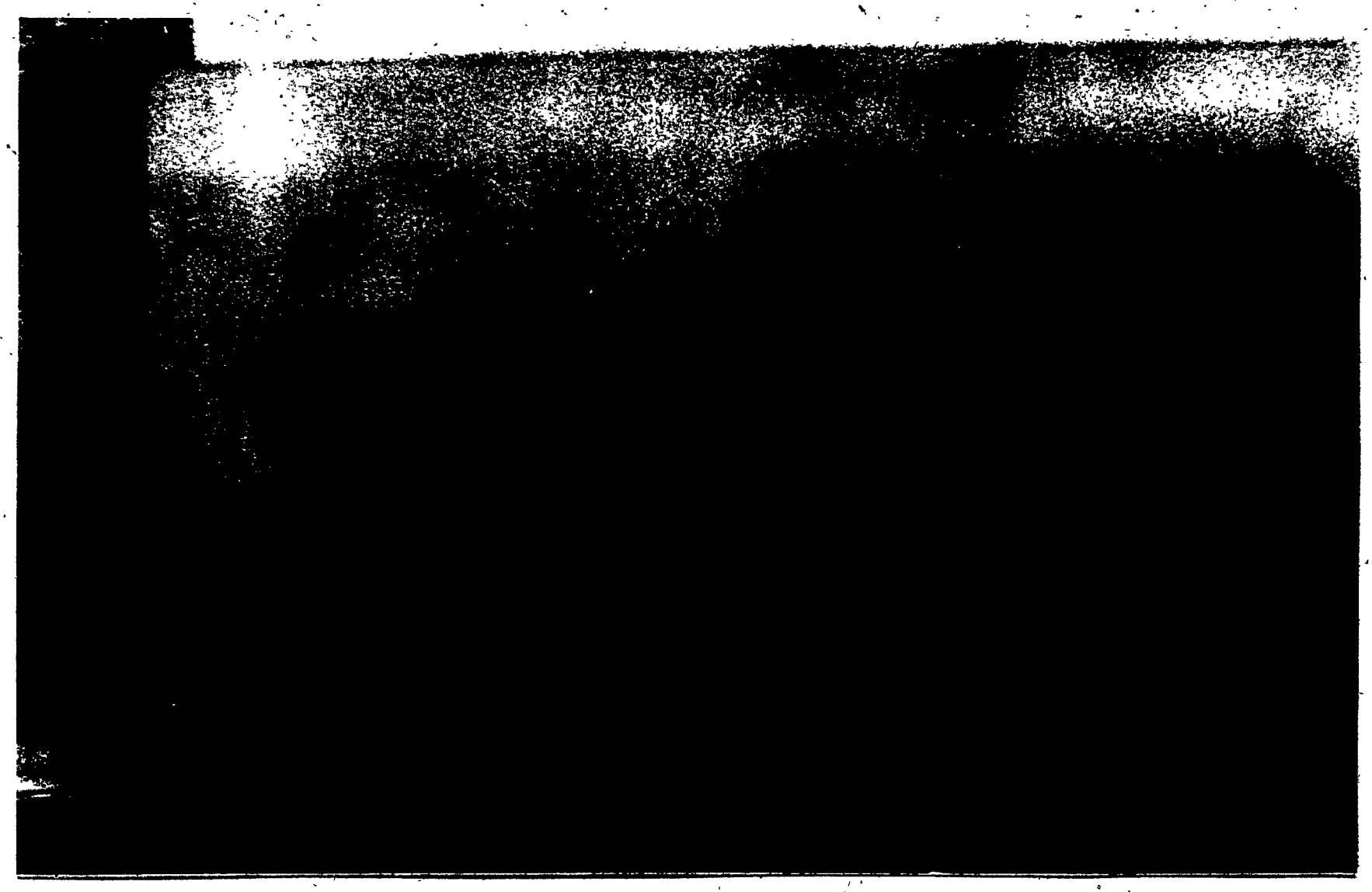

L = 28.5 in. H = 12 in.
Θ = 34° With Step
Sand Mixture

Fig. 2.7

Liquefaction Test 5

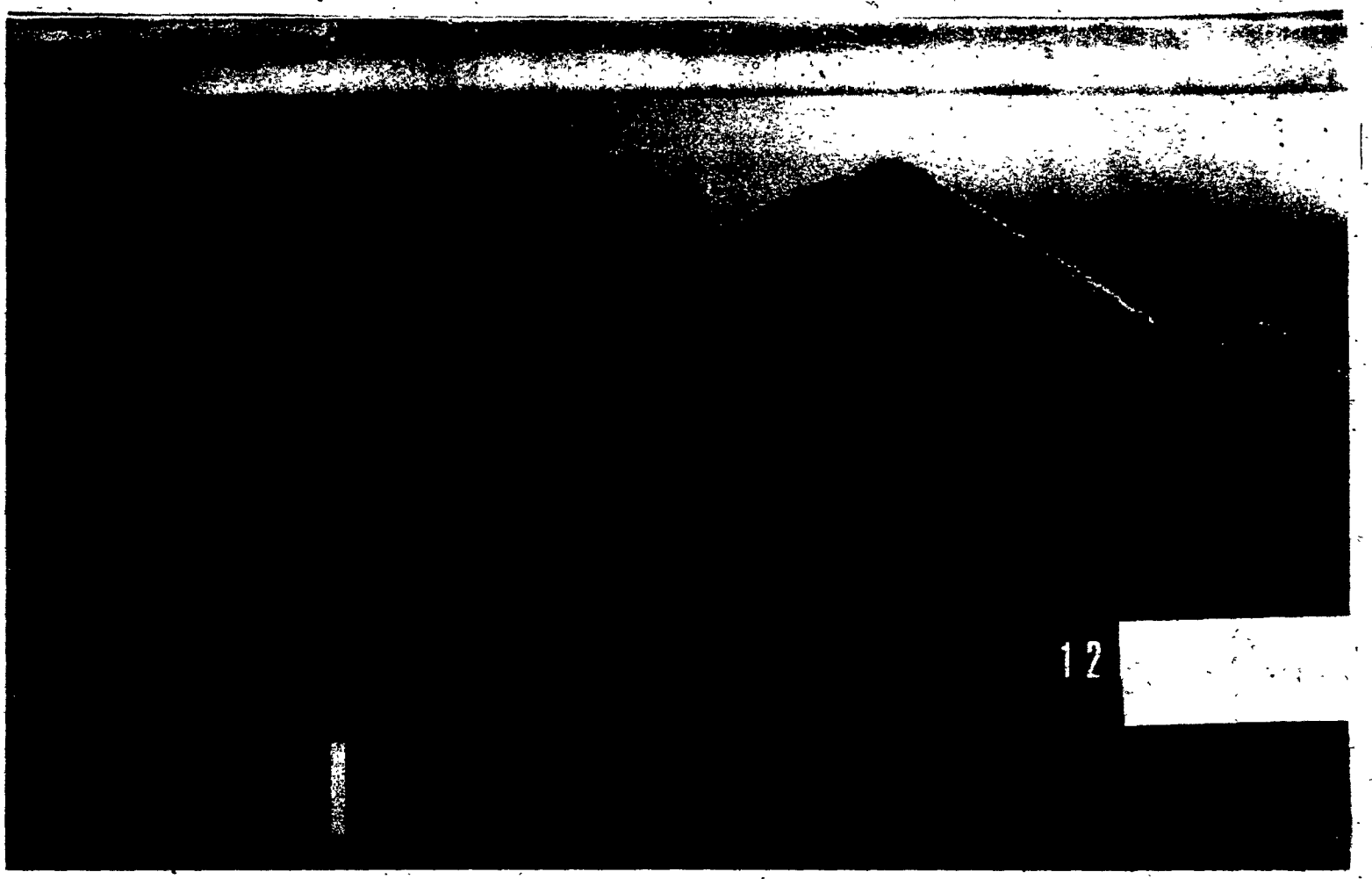

L = 29.5 in. H = 12 in.
Θ = 35° With Step
Sand Mixture

Fig. 2.8

Liquefaction Test 6

CHAPTER 3

ANALYSIS OF THE FLOW OF LIQUEFIED SAND DEPOSITS

3.1 Introduction

This chapter describes the analysis procedure used to study the mode of failure of liquefied sand deposits. Also presented in this chapter is a review of published literature on the behaviour of liquefied tailings and similar earth materials; a review of the available literature on the stress-strain rate relationships of non-Newtonian fluids, and a review of the Unsteady-Boundary-Layer Theory.

3.2 Literature review on the behavior of liquefied tailings and similar earth materials

The available literature on the flow behaviour of liquefied tailings is very limited. Some related work from various sources is reviewed in this section.

3.2.1 The Dam-Break Wave

This problem deals with the course of events following the sudden removal of a dam holding a semi-infinite body of water at rest. See Fig. 3.1

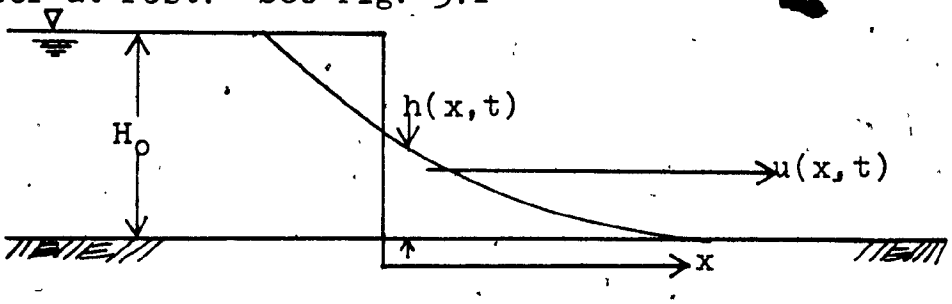

Fig. 3.1
The Dam-Break Problem

The classical solution for this problem was derived by Ritter (1892). He made the following assumptions:

a) The downstream bed is dry and horizontal.

b) The water behind the dam extends indefinitely.

c) Fluid frictional effects are negligible.

d) The pressure distribution in the flow is hydrostatic.

e) The dam is lost instantaneously.

f) The water particles on the free surface before the breach will continue to remain on the free surface during flow.

g) The channel is very wide.

Based on these assumptions, the mass conservation, and the one-dimensional momentum conservation equations (Saint Venant's equations) that govern the flow of fluids from behind the breached dam are:

$$\frac{\partial u}{\partial t} + u\frac{\partial u}{\partial x} + 2c\frac{\partial c}{\partial x} = 0$$

$$c\frac{\partial u}{\partial x} + 2\frac{\partial c}{\partial t} + 2u\frac{\partial c}{\partial x} = 0 \qquad \text{Eq. 3.1}$$

where:

$c = \sqrt{gh}$ = celerity

u = velocity of flow

h = flow depth

x = horizontal distance

t = time

g = acceleration due to gravity

H_o = dam height

the initial conditions being:

$$u(x,0) = 0$$
$$c(x,0) = 1 \quad \text{for } x<0 \qquad \text{Eq. 3.2}$$
$$c(x,0) = 0 \quad \text{for } x>0$$

with the following boundary conditions:

$$u(-1,t) = 0 \quad \text{for } t>0 \qquad \text{Eq. 3.3}$$
$$c(-1,t) = 1 \quad \text{for } t>0$$

The above problem is solved by the method of characteristics, and gives:

$$\left\{\frac{\partial}{\partial t} + (u+c)\frac{\partial}{\partial x}\right\}(u+2c) = 0 \quad \text{on } c^+ \qquad \text{Eq. 3.4}$$
$$\left\{\frac{\partial}{\partial t} + (u-c)\frac{\partial}{\partial x}\right\}(u-2c) = 0 \quad \text{on } c^-$$

where c^+ and c^- are two families of characteristics curves given by:

$$c^+ : \frac{dx}{dt} = u+c \qquad \text{Eq. 3.5}$$
$$c^- : \frac{dx}{dt} = u-c$$

The complete solution is presented in various textbooks of open channel hydraulics, among them, Henderson (1966).

After loss of the dam, there are three zones on the x,t plane, (see Fig. 3.2)

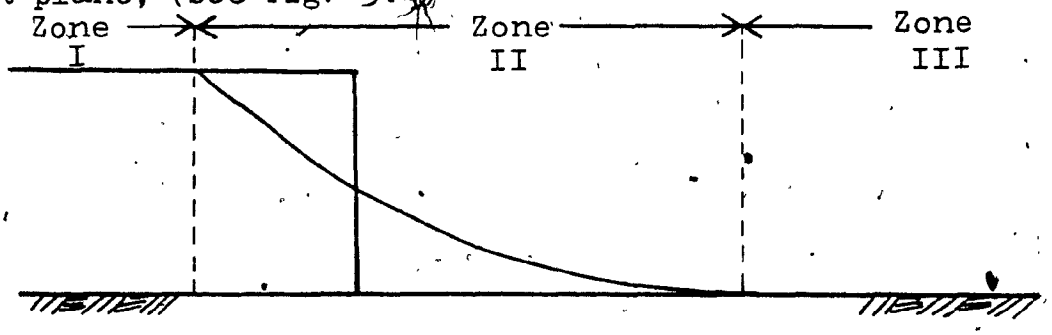

Fig. 3.2
Zones after loss of a Dam

Zone I is referred to as the quiet zone, within which the negative wave travels with a constant velocity $-c_o$, where $c_o = \sqrt{gH_o}$. In Zone III the depth of water is zero, and in Zone II the characteristics of the c^+ family are divergent. The positive wave travels in the downstream direction with a constant velocity $2c_o$.

Ritter's solutions to this problem using the method of characteristics are:

$$u = \frac{2}{3}\left(1 + \frac{x}{t}\right)$$

$$c = \frac{1}{3}\left(2 - \frac{x}{t}\right) \qquad \text{Eq. 3.6}$$

There are computer programs commercially available to determine the extent of flow movement once a water storage dam has failed. The resulting flow from the breach of such a dam is turbulent, and therefore boundary resistance is included in the analysis using an empirical Manning's n relationship. Unfortunately, these analysis-techniques cannot be used for flow failures of most tailings deposits because the nature of the flow of liquefied tailings is different from that of water, in that viscous frictional effects are appreciable in liquefied tailings.

3.2.2 Analyses of Turbulent Flow

This type of analysis is useful only in the study of flow of phosphate tailings, since all the other types of failures of tailings deposits are known to be laminar.

The analysis is carried out by introducing a turbulent resistance term in the Saint Venant's equations:

$$\frac{\partial u}{\partial t} + u\frac{\partial u}{\partial x} + 2c\frac{\partial c}{\partial x} + R\frac{u^2}{c^2} = 0$$

$$c\frac{\partial u}{\partial c} + 2\frac{\partial c}{\partial t} + 2u\frac{\partial u}{\partial x} = 0 \qquad \text{Eq. 3.7}$$

where:

$R = \frac{kh_r^{1/6}}{n}$ = Chezy Coefficient

k = constant = 1.489 for English units, and
1.0 for Metric units.

n = Manning's n

h_r = Hydraulic radius, which is the ratio of the water area to its wetted perimeter.

There are two methods for solving these equations:

A) Dressler's Method:

In this method a simple perturbation expansion is used to determine correction functions in the tip region of the flow, where the boundary resistance forces are of the same magnitude as the inertial forces. These solutions are:

$$u(x,t) = \frac{2}{3}(1+m) + Rth_1(m) + \ldots..$$

$$c(x,t) = \frac{1}{3}(2-m) + Rtk_1(m) + \ldots.. \qquad \text{Eq. 3.8}$$

where:

$$h_1(m) = \frac{-108}{7(2-m)^2} + \frac{12}{(2-m)} - \frac{8}{3} + \frac{8\sqrt{3}}{189}(2-m)^{3/2}$$

$$k_1(m) = \frac{6}{5(2-m)} - \frac{2}{3} + \frac{4\sqrt{3}}{135}(2-m)^{3/2}$$

$$m = \frac{x}{t}$$

B) Whitham's Method:

Where the tip region is treated as a boundary layer in which the equations are solved in an integrated form, and outside the boundary layer region, the inviscid dam break wave solutions for velocity and depth of flow are used.

The above procedures for analysis of turbulent flow dam break problems are simple and practical, but they cannot be used for analysis of flows on sloping beds or for analysis of flows in valleys of varying cross-sections.

The current procedures for inundation studies for water storage dams use finite difference computer solutions of St. Venant's equations.

3.2.3 Analysis of Laminar Flow

There are mainly two methods of treating the analysis of laminar flow, both take into consideration only viscosity but not yielding shear strength, and the solutions are applicable only to Newtonian fluids.

Therefore, these results cannot be directly used for the analyses of flow characteristics of liquefied tailings, or liquefied sand which have a threshold shear resistance as well as viscosity, and their stress-strain rate relationship is not linear.

These two methods are:

A) Tip Theory:

In this theory, the tip region of the flow can be studied separately and joined with the inviscid mainstream solutions

satisfying the requirements for mass-conservation and dynamic force equilibrium at the interface. The Tip Theory is based on an approximate treatment of the boundary layer in the tip region of the dam-break wave, using Pohlhausen's integration technique.

The solutions are:

$$u_T(t) = 2\sqrt{gH_o}\left(1 - 1.5938\left(\frac{\nu t}{H_o^2}\right)^{1/5}\right)$$

$$x(t) = 2\sqrt{gH_o}\,t\left(1-1.3282\left(\frac{\nu t}{H_o^2}\right)^{1/5}\right) \qquad \text{Eq. 3.9}$$

where:

ν = kinematic viscosity of fluid

H_o = dam height

t = time after dam break

B) Perturbation Method:

In this method, viscous effects are considered by adding a viscous effect term to Saint Venants equations:

$$\frac{\partial u}{\partial t} + u\frac{\partial u}{\partial x} + 2c\frac{\partial c}{\partial x} + R\frac{u}{c^4} = 0$$

$$c\frac{\partial u}{\partial x} + 2\frac{\partial u}{\partial t} + 2u\frac{\partial c}{\partial x} = 0 \qquad \text{Eq. 3.10}$$

where:

$$R = \frac{2\eta}{\gamma H_o}\sqrt{\frac{g}{H_o}}$$

The solutions for the above set of equations are valid only for wide horizontal channels and are given by:

$$u(x,t,R) = \frac{2}{3}(1+m) - \frac{216(1+m)Rt}{11(2-m)^4} + \frac{30Rt}{22(2-m)^3} - \frac{10Rt}{198}\left(2/3 - m/3\right)^{3/2} \qquad \text{Eq. 3.11.a}$$

$$c(x,t,R) = \frac{1}{3}(2-m) + \frac{27(1+m)Rt}{11(2-m)^4} + \frac{21\,Rt}{22(2-m)^3} + \frac{7Rt}{198}(2/3 - m/3)^{3/2} \qquad \text{Eq. 3.11.b}$$

A third method of analysis of laminar flow of liquefied tailings was developed by Jeyapalan, (1980). He considers the effects of a yielding shear strength by adding such term to the Saint Venant's equations:

$$\frac{\partial u}{\partial t} + u\frac{\partial u}{\partial x} + 2c\frac{\partial c}{\partial x} + R\frac{u}{c^4} + \frac{S}{c^2} = 0$$

$$c\frac{\partial u}{\partial x} + 2\frac{\partial c}{\partial t} + 2u\frac{\partial c}{\partial x} = 0 \qquad \text{Eq. 3.12}$$

where:

$$R \equiv \frac{2\eta_p}{\gamma H_o}\sqrt{\frac{g}{H_o}}$$

$$S = \frac{\tau_y}{\gamma H_o}$$

The solutions are given by:

$$u(x,t,R) \cong \frac{2}{3}(1+m) - \frac{27\,St}{7(2-m)^2} - \frac{216(1+m)Rt}{11(2-m)^4} + \frac{30Rt}{22(2-m)^3} - \left(-\frac{3St}{7} + \frac{10Rt}{198}\right)\left(\frac{2}{3} - \frac{m}{3}\right)^{3/2} \qquad \text{Eq. 3.13}$$

$$c(x,t,R) \cong \frac{1}{3}(2-m) - \frac{3St}{10} + \frac{27(1+m)Rt}{11(2-m)^4} + \frac{21Rt}{22(2-m)^3} - \left(-\frac{3St}{7} - \frac{7Rt}{198}\right)\left(\frac{2}{3} - \frac{m}{3}\right)^{3/2}$$

The procedure for calculating the free surface profile at any time after the dam breach is shown in Fig.3.3. The disturbed portion of the fluid is subdivided into two zones. Zone II occupies the region from the position of maximum flow velocity to the zone of quiet, whereas Zone I represents the

tip region, in which the velocity is assumed to be constant.

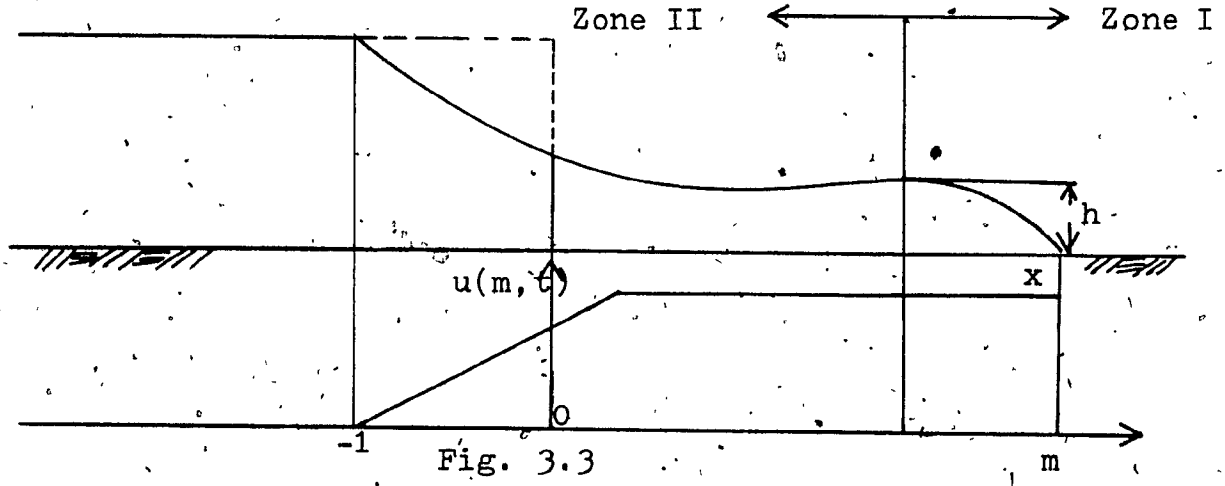

Fig. 3.3

Procedure for Calculating Free Surface Profile

The free surface profile is given by:

$$h(x,t) = c^2(x,t)H_o \qquad \text{for Zone II}$$

$$-\frac{dh}{dx} = \frac{2\eta u}{\gamma h^2} \qquad \text{for Zone I, where} \qquad \text{Eq. 3.14}$$

the viscous resistance and pressure gradients are approximately equal.

3.3 Review of the literature on non-steady boundary layer theory

The most common example of non-steady boundary layers occurs when the motion is started from rest. When this happens both the body and the fluid have zero velocities up to a certain instant of time. The motion begins at that instant and it can be considered that either the body is dragged through the fluid at rest, or that the body is at rest and the external fluid motion varies with time. In this latter case an initially very thin boundary layer is formed near the body and the transition from the velocity of

the body to that in the external flow takes place across it. Immediately after the start of the motion the flow in the whole fluid space is irrotational and potential with the exception of a very thin layer near the body. The thickness of the boundary layer increases with time, and it is important to investigate at which instant separation (reverse flow) first occurs as the boundary layer continues to build up.

The fundamental equations of non-steady boundary layer are given in Schlichting (1979), and they will be presented below for two-dimensional flows:

$$\frac{\partial u}{\partial t} + u\frac{\partial u}{\partial x} + v\frac{\partial u}{\partial y} = \frac{1}{\rho}\frac{\partial p}{\partial x} + \frac{\partial^2 u}{\partial y^2}$$

$$\frac{\partial u}{\partial x} + \frac{\partial v}{\partial y} = 0 \qquad \text{Eq. 3.15}$$

the boundary conditions being:

$$\text{when } y = 0, \quad u = v = 0$$

$$\text{when } y = \infty, \quad u = U(x,t) \qquad \text{Eq. 3.16}$$

the pressure impressed on the body follows from the non-steady Bernoulli's equation:

$$-\frac{1}{\rho}\frac{dp}{dx} = \frac{\partial U}{\partial t} + U\frac{\partial U}{\partial x} \qquad \text{Eq. 3.17}$$

where:

$U(x,t)$ denotes the velocity of the edge of the boundary layer.

The integration of the non-steady boundary layer equations (3.15 - 3.17) can be carried out in most cases by a process of successive approximations, the method being based on the following physical reasoning. In the first

instant, after the motion has started from rest, the boundary layer is very thin and the viscous term $\nu \frac{\partial^2 u}{\partial y^2}$ is very large, whereas the convective terms retain their normal values. The viscous term is then balanced by the non-steady acceleration $\frac{\partial u}{\partial t}$ together with the pressure term in which, at first, the contribution of $\frac{\partial U}{\partial t}$ is of importance. Selecting a system of coordinates which is at rest with respect to the body and assuming that the fluid moves with respect to the body at rest, we can make the assumption that the velocity is composed of two terms:

$$u(x,y,t) = u_o(x,y,t) + u_1(x,y,t) \qquad \text{Eq. 3.18}$$

Under these conditions, the first approximation, u_o, satisfies the differential equation:

$$\frac{\partial u_o}{\partial t} - \nu \frac{\partial^2 u_o}{\partial y^2} = \frac{\partial U}{\partial t} \qquad \text{Eq. 3.19}$$

with the boundary conditions:

$$\begin{aligned} &\text{at } y = 0, \quad u_o = 0 \\ &\text{at } y = \infty \quad u_o = U(x,t) \end{aligned} \qquad \text{Eq. 3.20}$$

The equation for the second approximation, u_1, is obtained with reference to Eq. 3.15, in which the convective terms are calculated from u_o and in which the convective pressure term can now be taken into consideration. Hence, we have:

$$\frac{\partial u_1}{\partial t} - \frac{\partial^2 u_1}{\partial y^2} = U \frac{\partial U}{\partial x} - u_o \frac{\partial u_o}{\partial x} - v_o \frac{\partial u_o}{\partial y} \qquad \text{Eq. 3.21}$$

with the boundary conditions being:

$$u_1 = 0 \quad \text{at } y = 0$$
$$u_1 = 0 \quad \text{at } y = \infty \qquad \text{Eq. 3.22}$$

In addition, we have the continuity equation for u_o, v_o and u_1, v_1. Higher-order approximations u_2, u_3, ... can be obtained in a similar manner.

3.3.1 Motion started impulsively from rest, growth of the boundary layer.

The fluid is at rest, and the solid body is set impulsively in motion, at t = 0, with a constant velocity, the motion is considered relative to the solid body. The boundary layer equation is:

$$\frac{\partial u}{\partial t} + u\frac{\partial u}{\partial x} + v\frac{\partial u}{\partial y} = U_1\frac{\partial U_1}{\partial x} + \nu\frac{\partial^2 u}{\partial y^2} \qquad \text{Eq. 3.23}$$

with the conditions:

$$t \leqslant 0, \quad u = 0$$
$$t > 0, \quad u = U_1(x) \qquad \text{Eq. 3.24}$$

where:

$U_1(x)$: the velocity corresponding to the inviscid flow.

At the beginning of the motion the boundary layer is of zero thickness, therefore, the convection terms and $U_1\frac{\partial U_1}{\partial x}$ can be disregarded; whence, to first approximate,

$$\frac{\partial u_o}{\partial t} = \nu\frac{\partial^2 u_o}{\partial y^2} \qquad \text{Eq. 3.25}$$

where the boundary conditions are:

$$u_o = 0 \quad \text{at } y = 0$$

$$u_o = U_1(x) \quad \text{at } y = \infty \qquad \text{Eq. 3.26}$$

Equation 3.25 is the familiar one-dimensional heat conduction equation whose solution has been worked out as:

$$u_o = \frac{2\,U_1}{\sqrt{\pi}} \int_0^{\eta} e^{-\eta^2}\, d\eta \qquad \text{Eq. 3.27}$$

where:

$$\eta = \frac{y}{2(\nu t)^{\frac{1}{2}}}$$

the velocity v_o, which can be found from (3.27) and the equation of continuity, vanishes at $y = 0$; it does not tend, however, to zero for $y = \infty$, but increases with y; for moderate values of η, v is of the order of $(\nu t)^{\frac{1}{2}}$.

To find the next approximation, a stream function $\psi(x,y,t)$ is introduced such that:

$$u = \frac{\partial \psi}{\partial y} \qquad v = -\frac{\partial \psi}{\partial x} \qquad \text{Eq. 3.28}$$

and ψ is expressed in powers of t, namely:

$$\psi(x,y,t) = 2(\nu t)^{\frac{1}{2}} \left\{ u_1 f_o(\eta) + t U_1 \frac{dU_1}{dx} f_1(\eta) + \ldots \right\}$$

Eq. 3.29

From equations 3.29 and 3.25, the equation for f_o is:

$$f_o''' + 2\eta f_o'' = 0 \qquad \text{Eq. 3.30}$$

with the boundary conditions:

$$f_o(0) = f_o'(0) = 0; \qquad f_o'(\infty) = 1 \qquad \text{Eq. 3.31}$$

which corresponds to the solution (3.27).

For f_1, and from (3.23) and (3.21),

$$f_1''' + 2\eta f_1'' - 4f_1' = 4(f_o'^2 - f_o f_o'' - 1) \qquad \text{Eq. 3.32}$$

the boundary conditions being:

$$f_1(0) = f_1'(0) = 0; \qquad f_1'(\infty) = 0 \qquad \text{Eq. 3.33}$$

the solution worked out by Blasius is:

$$f_1' = \frac{6\eta}{\pi}\int_{\infty}^{\eta} e^{-\eta^2}\,d\eta + \frac{2}{\pi}(2\eta^2 - 1)\left[\int_{\infty}^{\eta} e^{-\eta^2}\,d\eta\right]^2 + \frac{2}{\pi}e^{-2\eta^2} + \frac{1}{\sqrt{\pi}}\eta e^{-\eta^2} - \frac{4}{\sqrt{\pi}}\int_{\infty}^{\eta} e^{-\eta^2}\,d\eta - \frac{4}{3\pi}e^{-\eta^2} + \left(\frac{3}{\sqrt{\pi}} + \frac{4}{3\sqrt{\pi}}\right) x \left[\left(\eta e^{-\eta^2} + (2\eta^2 + 1)\int_{\infty}^{\eta} e^{-\eta^2}\,d\eta\right)\right] \qquad \text{Eq. 3.34}$$

whence,

$$u = u_o f_o' + u_1 \frac{du_1}{dx} f_1 + \ldots\ldots \qquad \text{Eq. 3.35}$$

The condition for separation is: $\frac{\partial u}{\partial y} = 0$ at $\eta = 0$; whence the time of separation can be calculated from:

$$1 + \left(1 + \frac{4}{3\pi}\right) t_s \frac{du_1}{dx} = 0 \qquad \text{Eq. 3.36}$$

and the distance travelled from the commencement of the motion is:

$$s = u_o t_s \qquad \text{Eq. 3.37}$$

3.4 Literature review on the stress-strain rate relationship of non-Newtonian fluids

For an elastic solid body, the shearing stress is proportional to the strain (Hooke's Law) and the constant of proportionality is the modulus of rigidity, G.

$$\tau = G\gamma \qquad \text{Eq. 3.38}$$

whereas in the case of fluids, experience shows that the shearing stress is proportional to the rate of change of

strain, $\frac{d\gamma}{dt}$, or $\dot{\gamma}$. The constant of proportionality being the viscosity, μ, a characteristic constant of the material at a given temperature and pressure.

For Newtonian fluids, this relationship is linear and given mathematically and graphically by Eq. 3.39 and Fig. 3.4 respectively.

$$\tau = \mu \frac{d\gamma}{dt} \quad \text{or} \quad \tau = \mu \dot{\gamma} \qquad \text{Eq. 3.39}$$

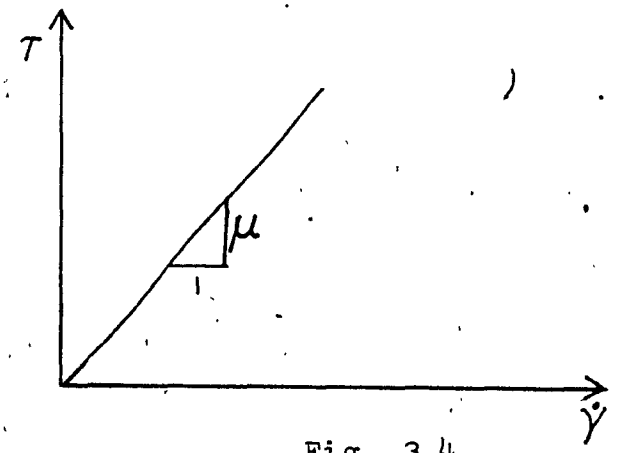

Fig. 3.4

Stress-strain rate curve for a Newtonian fluid

In the case of non-Newtonian fluids, however, the functional relationship is non-linear. In fact, many models can be used for the description of non-Newtonian flow characteristics and the important criterion is that of the degree to which they are able to fit the available data. Some of these methods will be presented below. The list is exhaustive as new models continue to be developed. Most of them are semi-empirical or have been developed from molecular theories.

a) The Ostwald-de Waele Model, sometimes referred to as the "power law". However, it is not a law, only an attempt at empirical curve fitting with maximum simplicity. It is the most criticized, and most widely used equation in all rheology. It has the advantage of being the simplest, easiest to manipulate, and suitable for use as an interpolation formula even though it may fail to fit the total range of experimental data for some materials, the expression can be very useful for a two-constant fit of rheological data over a restricted range of shear rate. Its mathematical representation is given by Eq. 3.40. The stress-strain rate curve is shown on Fig. 3.5.

$$\tau = K\dot{\gamma}^{n} \qquad \text{Eq. 3.40}$$

where:

K and n are material parameters which in general vary with pressure and temperature (and composition in case of mixtures) and they can be determined empirically.

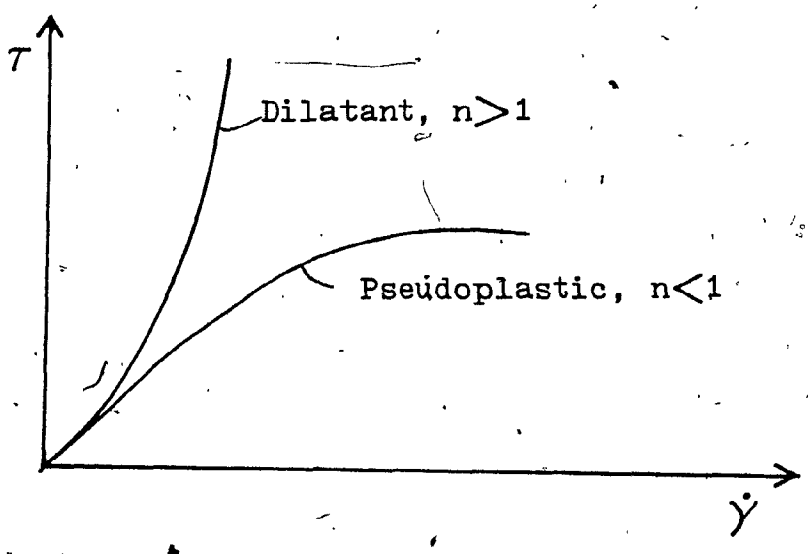

Fig. 3.5

Stress-Strain Rate Curve for the Ostwald-de Waele Model

b) The Ellis Model, which is only a modification of the Ostwald-de Waele model. Its functional relationship is given by Eq. 3.41, and Fig. 3.6.

$$\tau = \mu_{eff}\dot{\gamma} \qquad \text{Eq. 3.41}$$

where:

$\frac{1}{\mu_{eff}} = \frac{1}{\mu_o}\left[1+\left(\frac{\tau}{\tau_{\frac{1}{2}}}\right)^{\frac{1-n}{n}}\right]$; and $\tau_{\frac{1}{2}}$ is the shear stress at $\mu_{eff} = \frac{1}{2}\mu_o$

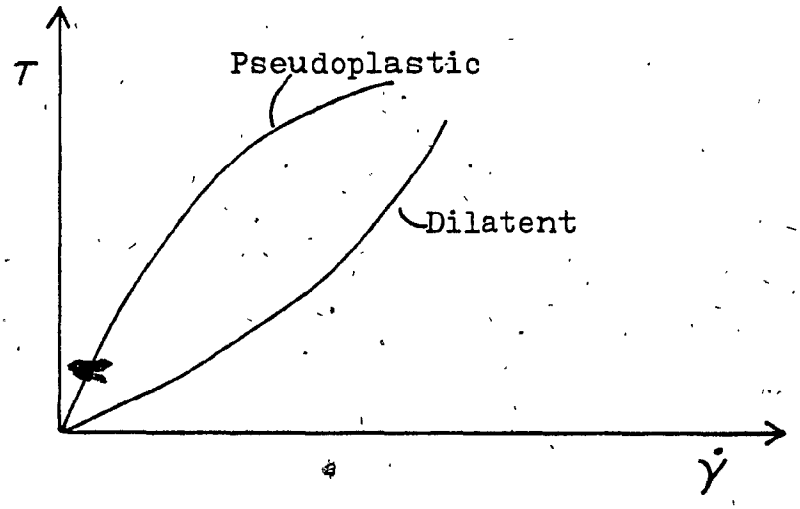

Fig. 3.6

Stress-Strain Rate Curve for Ellis Model

c) Eyring Model. The relationship for this model is shown below.

$$\tau = A \sinh^{-1}\left(\frac{\dot{\gamma}}{B}\right) \qquad \text{Eq. 3.42}$$

where:

A and B are material constants.

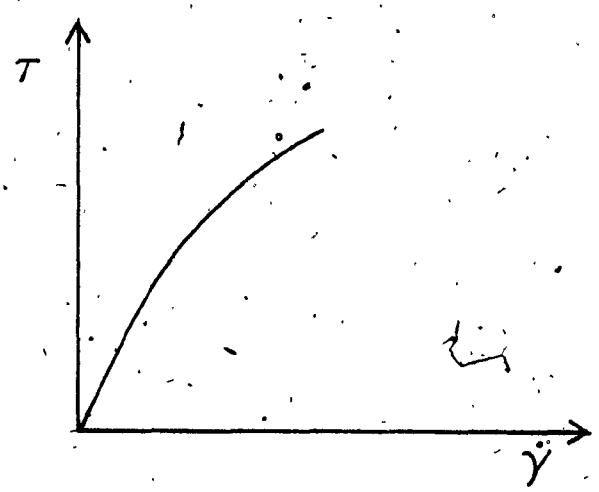

Fig. 3.7

Stress-Strain Rate Curve for Eyring Model

e) The Bingham Plastic Model. This model incorporates the idea of a finite yield stress which is that stress to be overcome before the material will sustain a non-zero rate of strain. Yielding fluids are really part fluid and part solid, for this reason this model has been widely used in the study of liquefied sands, and will be used in this reseach project.

The expression for the stress-strain rate is given by equation 3.43.

$$\tau = \tau_y + \mu_p \dot{\gamma} \quad \text{for} \quad \tau > \tau_y$$

$$\gamma = 0 \quad \text{for} \quad \tau < \tau_y \qquad \text{Eq. 3.43}$$

where:

τ_y : Bingham yield strength

μ_p : Plastic Viscosity

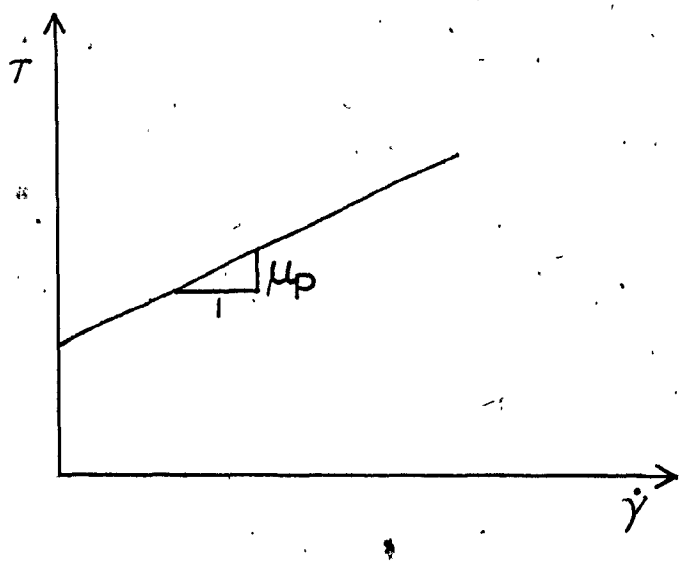

Fig. 3.8

Stress-Strain Rate Curve for Bingham Plastic Model

3.5 Analysis of Test Results

From the flume experiments conducted as part of this research study, it was found that the perturbation technique developed by Jeyapalan (1980) for the analysis of laminar flow of liquefied tailings was applicable and conforms with the results presented in Chapter 2.

Therefore, the governing equations are given by Eq. 3.12, whose solution for a horizontal bed was derived using the perturbation technique and the Bingham Plastic model, and are given in Eq. 3.13.

By calculating the velocity over a time interval, a new displacement and the resulting flow profile can be calculated. The updated flow profile can then be used to calculate the tip velocity for the subsequent time interval. If this procedure is repeated until the calculated tip velocity is found to be

zero, then at this stage the flow is considered "frozen".

The analytical results can be presented in the form of prediction charts based on dimensionless resistance parameters:

$$R = \frac{2\eta_p}{\gamma H_o}\sqrt{g/H_o} \qquad \text{and,} \qquad S = \frac{\tau_y}{\gamma H_o}$$

Typical predictive charts are shown on Figs. 3.9 and 3.10.

An example is presented below to illustrate the use of these charts.

Consider,

$H_o = 60$ ft.

$\gamma = 110$ lb/ft^3

$\eta_p = 25$ lb sec/ft^2

$\tau_y = 25$ lb/ft^2

then,

$$R = \frac{2(25)}{110(60)}\sqrt{\frac{32.2}{60}} = 0.0055$$

and $$S = \frac{25}{110(60)} = 0.0038$$

from Fig. 3.9, the dimensionless inundation distance, x_f: 31, and from Fig. 3.10, the dimensionless freezing time, t_f: 81.

To find the dimensional variables, we perform the following calculations:

$x_f^* = x_f H_o = 1860$ ft.

$t_f^* = t_f\sqrt{H_o/g} = 110$ sec.

and,

$$u^* = \left(\frac{x_f}{t_f}\right) = 16.91 \text{ ft/sec}$$

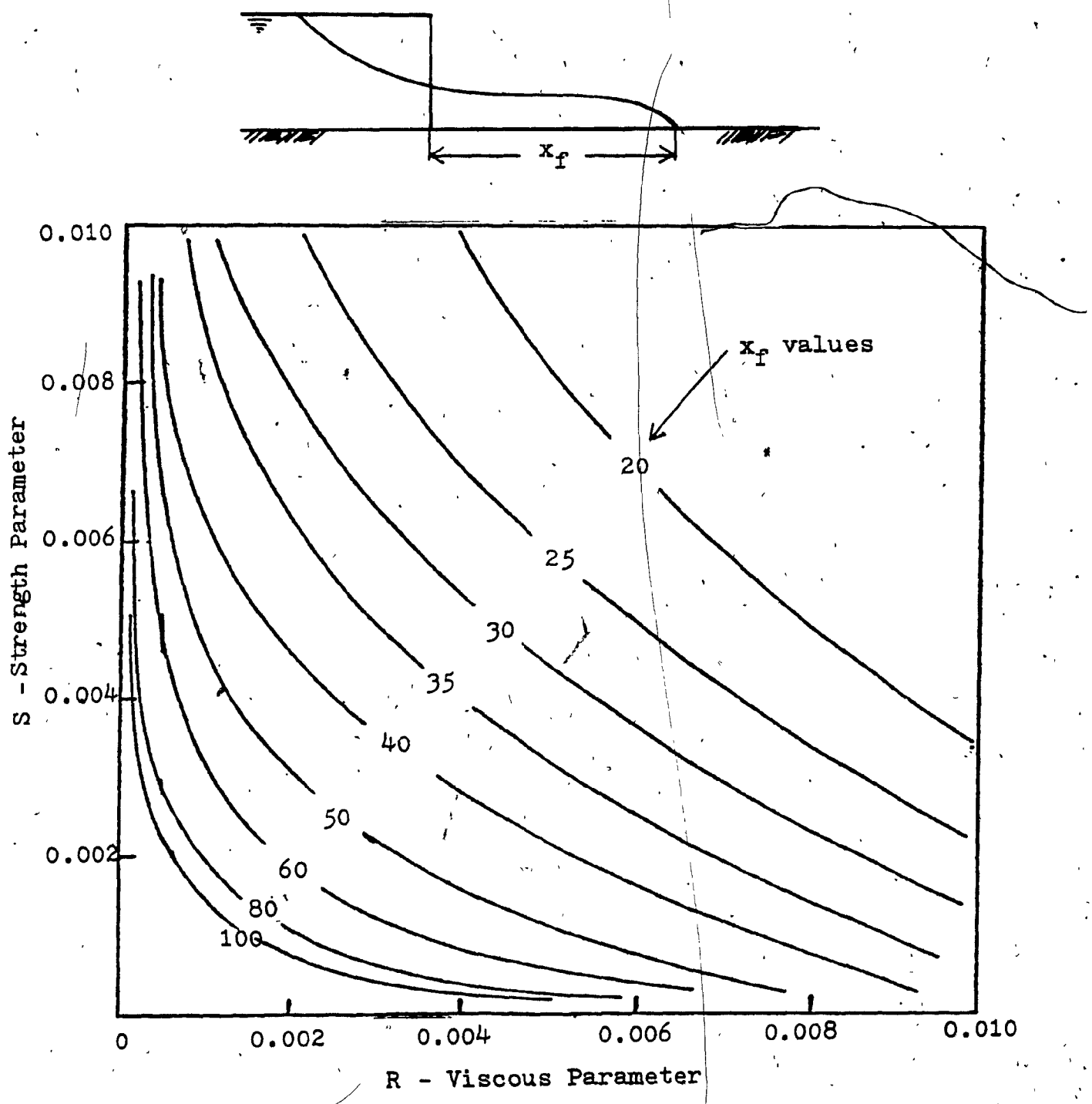

Fig. 3.9

Variation of Inundation Distance with Resistance
Source: Jeyapalan, (1980)

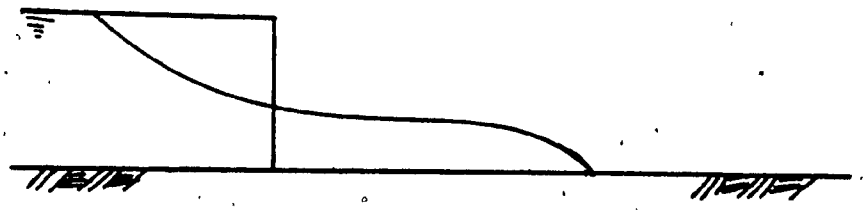

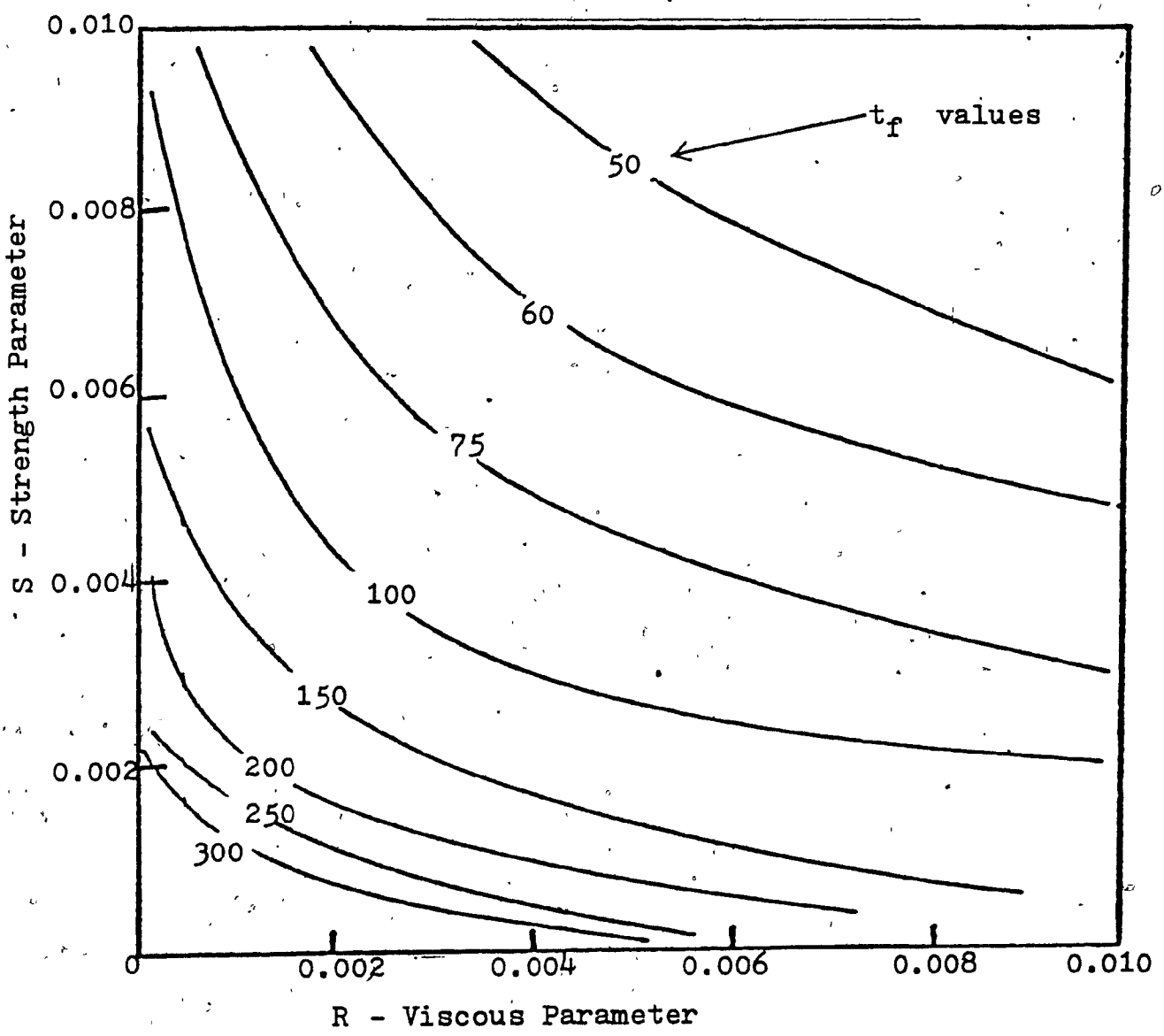

Fig. 3.10

Variation of Freezing Time with Resistance Parameters
Source: Jeyapalan, (1980)

CHAPTER 4

HYDRAULIC FRACTURING TESTS

4.1 Introduction

This chapter will describe a series of tests on hydraulic fracturing of clays. The details of the test material, the description of the tests and results will be presented as well.

4.2 Test Material

The soil used in this work was a Labrador clay of liquid limit = 35%, plastic limit = 25%, and plasticity index = 10%. According to the Unified Classification System, this clay can be classified as CL.

4.3 Description of Tests

The tests apparatus is shown schematically in Fig. 4.1. The procedure followed is presented below.

A piezometer made of copper tubing 0.315 in. inside diameter was used. Inside the piezometer, a plunger was provided to prevent the clay from filling the tubing when this is driven into the clay mass.

The actual driving of the piezometer into the soil was carried out by two different procedures without any evident difference in the results. These methods were:

a) To continuously drive the piezometer into the soil by hand.

b) To apply a 5-lb. weight on top of the piezometer

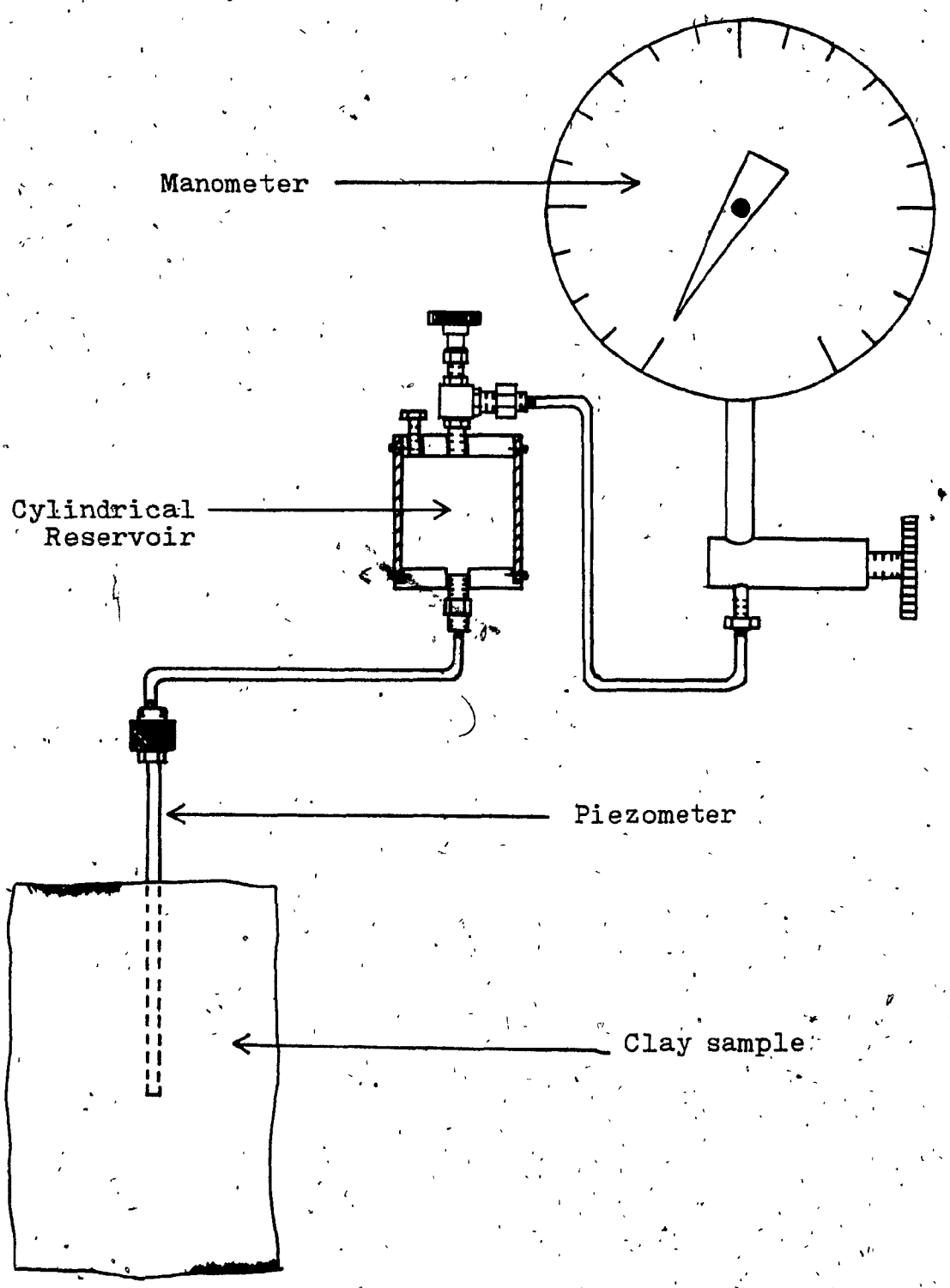

Fig. 4.1

Hydraulic Fracturing Set-up

so that it penetrates into the soil very slowly.

In both cases the piezometer was driven until the desired depth was attained, which in most tests was from 6 to 7 in.

Once the piezometer reached the required depth, the plunger was removed, and the piezometer was filled with oil coming from a cylindrical reservoir connected to the piezometer through plastic tubing.

The cylindrical reservoir was provided with a bleeder valve which was opened to ensure that air was not entrapped into the system. This reservoir was also connected to a manometer which measured the pressure, in pounds per square inch, at which the test was carried out.

The hydraulic fracturing test was performed by gradually increasing the hydraulic pressure in the piezometer using the manometer from the triaxial equipment until the soil fractured.

Once the test was completed, all the flows were cut-off, the valves were closed, and the fittings untightened. In general, the separation of the sample into two pieces was done quite easily after the sample had failed and then the piezometer was removed.

From the separated pieces of the sample, the cracks were observed and studied.

4.4 Test Results

Some typical results are illustrated on Figs. 4.2 and 4.3

Fig. 4.2

Hydraulic Fracturing Test Sample 1

Fig. 4.3

Hydraulic Fracturing Test Sample 2

CHAPTER 5

ANALYSIS OF A SPECIAL MODE OF INSTABILITY OF CLAYS DUE TO HYDRAULIC FRACTURING

5.1 Introduction

This chapter will present the analysis procedure to study a special mode of instability of clays due to Hydraulic Fracturing. A review of published literature on hydraulic fracturing and its diverse utilizations will be discussed. In addition, a review of the Mindlin formulation which is used in the analysis of the problem will be dealt with briefly.

5.2 Literature review on hydraulic fracturing

The first few lines of this section will describe what hydraulic fracturing is.

If liquid is pumped into a piezometer to a sufficient pressure, cracking occurs in the soil around the piezometer tip when the liquid pressure is large enough to cause tensile stresses in the soil next to the piezometer. This is known as hydraulic fracturing.

5.2.1 Hydraulic fracturing applied to rock formations

The method of hydraulic fracturing applied to rock formations is a well known technique and has been used by the petroleum industry since 1949. The oil industry recognized that the productivity of a well could be increased by increasing the permeability of the formation.

Prior to the use of the hydraulic fracturing technique, the petroleum industry utilized explosives, acidizing agents, and other methods to improve the productive ability of oil and gas wells. But, it was thought that another artificial means were required particularly for wells which produced from formations which did not react readily with acids. Therefore, the hydraulic fracturing process, "Hydrafrac", was developed and it was applicable to any type of formation. The method was also applied to gas and water injection wells, wells used for solution mining of salts and, with some modification, to water wells and sulphur wells. (Clark, 1949).

The process is still used and consists of the following steps:

a) Formation breakdown: This is done by injecting a viscous liquid, or gel, (oil, gasoline) containing a granular material (sand) for a propping agent, under high hydraulic pressure to fracture the formation.

b) Breaking down the viscosity of the gel by injecting a gel-breaker solution and then after several hours, putting the well back on production. The gel-breaker causes the viscous liquid to change from a high to a low viscosity so that it may be readily displaced from the formation.

The sequence of steps is shown diagramatically in Fig. 5.1.

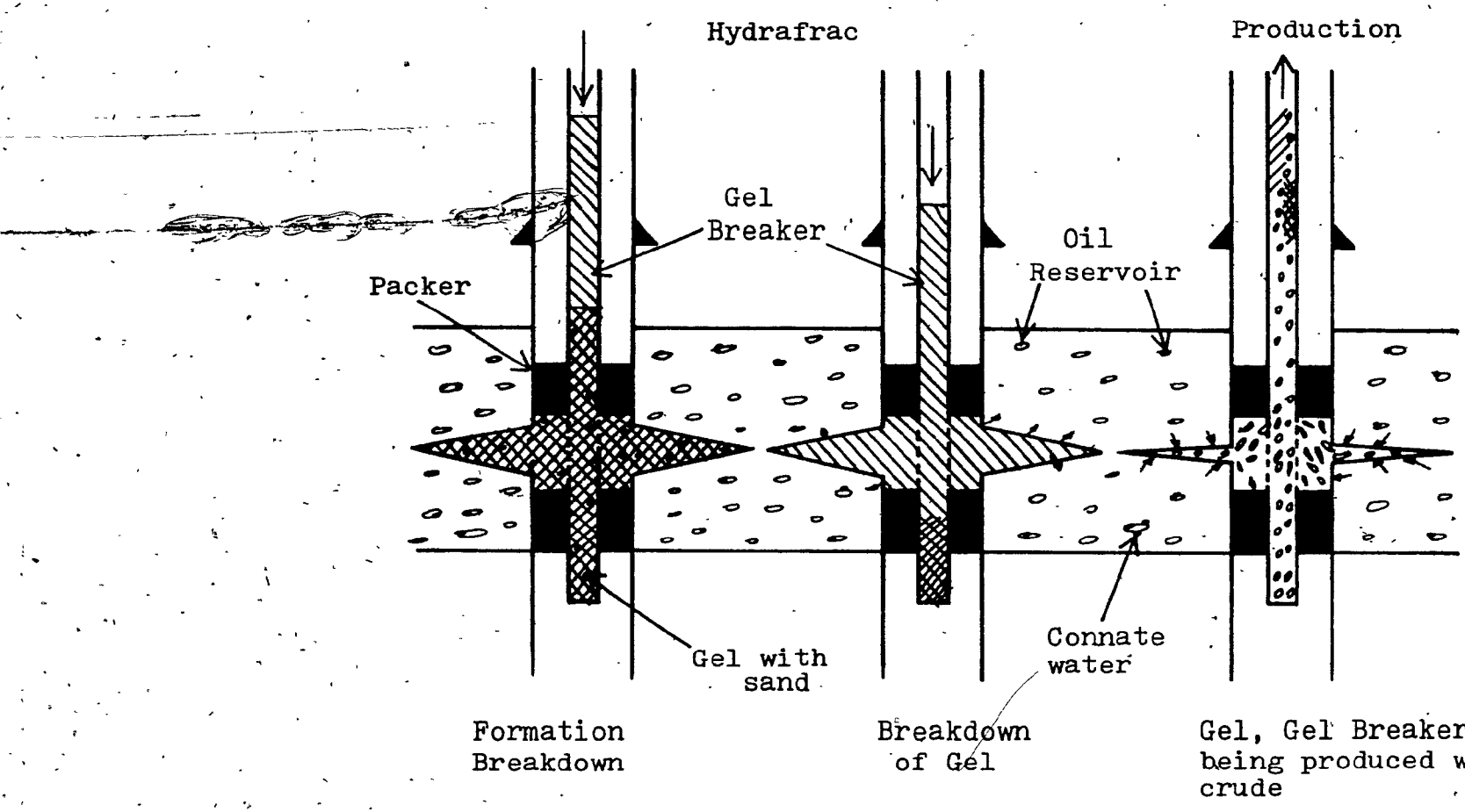

Fig. 5.1
Sequence of Steps in Hydrafrac Process

5.2.2 Hydraulic fracturing applied to measure the in-situ lateral pressures in clay

Although hydraulic fracturing has long been used to determine the modulus of rigidity, G, of the rock around a borehole or a tunnel, its use to measure the in-situ lateral pressures in clay is relatively recent.

The idea of using the hydraulic fracturing method in soil mechanics was conceived by Bjerrum and Andersen in 1972 while interpreting results from ordinary in-situ permeability tests in clays. Basically, they discovered that because the soil that they were testing had a low permeability, there was a temptation to use high pressures in order to give adequate flow readings within a reasonable time. This led to very false results owing to cracking in the soil around the piezometer tip when the water pressure got large enough to cause tensile stresses in the soil next to the piezometer. Up to this point, this danger was not generally recognized by geotechnical engineers.

Bjerrum and Andersen did a theoretical analysis of the problem and they concluded that the excess critical water pressure required to produce a fracture was related to the in-situ effective stresses, which were σ_o in a vertical and $K_o \sigma_o$ in a horizontal direction (where σ_o=effective overburden pressure=γD; and K_o=coefficient of earth pressure at rest). They also showed that if K_o was greater than 1.0 (i.e. over-consolidated clay), a horizontal crack will appear, and if K_o was less than 1.0 (i.e. normally consolidated clay), a vertical crack will form. They also found that the critical waterpressure

was dependent on the tensile strength of the soil, and on stress changes occurring in a thin zone in the soil close to the piezometer during its installation. So, they considered that the disturbance around the piezometer might lend considerable uncertainty if evaluating the horizontal effective stress by measuring the water pressure required to fracture the soil, therefore they decided that when a crack first appeared, the water pressure at which it closes again might be more reliable as an evaluation of the lateral stresses in the ground. If σ_o and the initial pore water pressure were known, then they could calculate K_o. They emphasized that the method was valid only for normally consolidated clays because if K_o is larger than 1.0 and a horizontal crack develops, the method will measure the weight of the overburden and not the in-situ lateral stress. A sketch of the field apparatus is shown in Fig.5.2 and the procedure is given in Bjerrum and Andersen (1972).

After the hydraulic method (to determine the coefficient of earth pressure at rest, K_o) was outlined, other procedures like the Total Stress Cell Method, the Conventional Pressuremeter, the Self-boring Pressuremeter, and the Camkometer were developed. Even though the hydraulic fracturing test is attractive for its simplicity and for its apparent good performance in the cases reported by Bjerrum and Andersen, the method is associated with major problems related, among other factors, to the clay disturbance caused by the introduction of the piezometer, and the basic assumption in the determination of K_o which says: "that fracture in the soil is con-

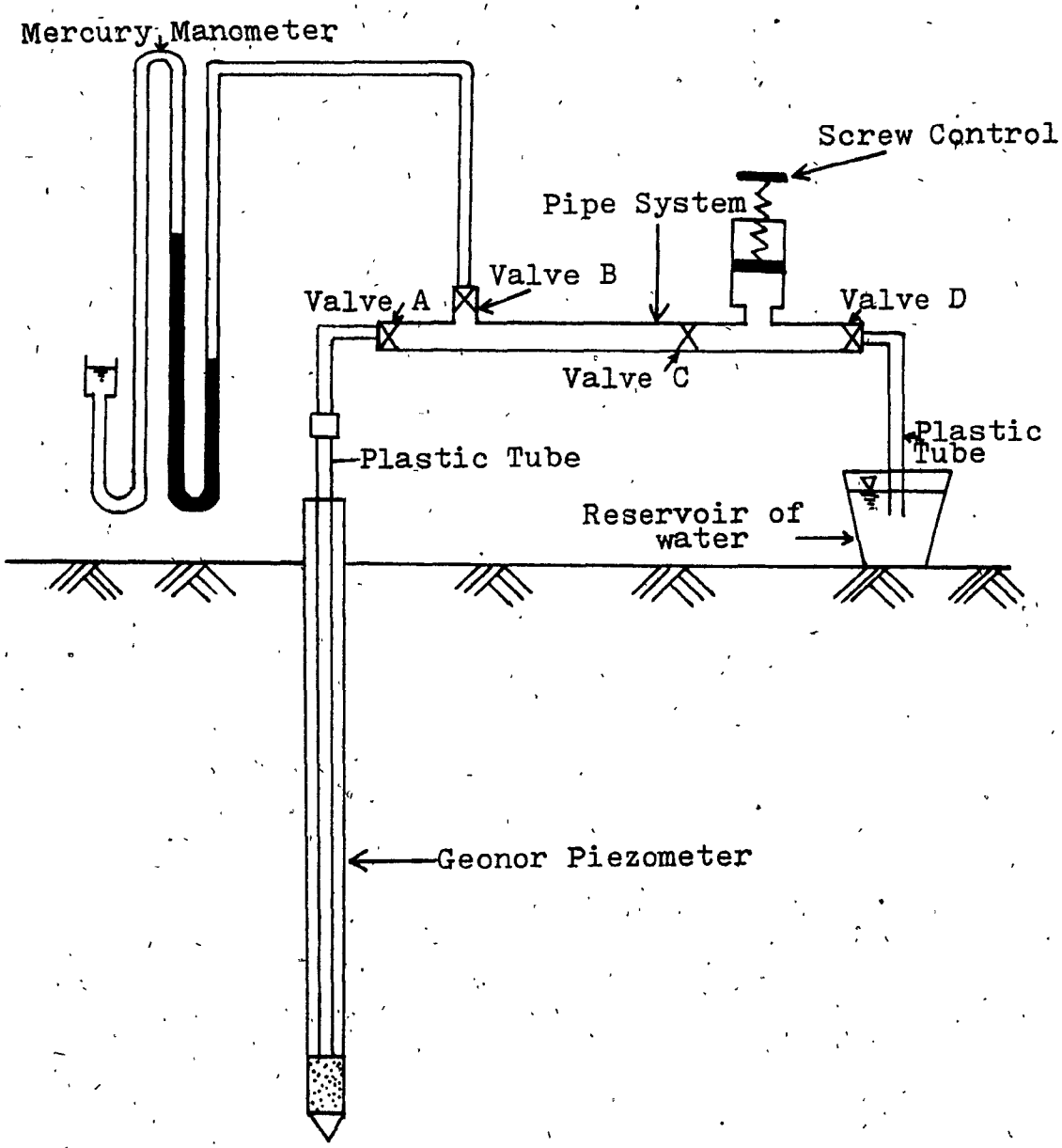

Fig. 5.2
Hydraulic Fracturing Field Apparatus

trolled by the in-situ state of stress only". This assumption is not necessarily correct for natural clays.

5.2.3 Hydraulic fracturing in zoned dams

Prior to 1970 there was no mention of the hydraulic fracturing concept for embankment dams in the literature, and little or no discussion or recognition of the phenomenon among geotechnical engineers. The last several years, however, have seen a complete change, with wide acceptance that hydraulic fracturing is not only possible but that the conditions conducive to its development exist frequently in dams.

The possible development of cracks in the cores of zoned dams (soft core and stiff shell, for example) is one of the major problems confronting the dam engineer. The hydraulic fracturing, or the formation of hydraulically induced cracks in the core, can occur when the water pressure at a given depth exceeds the total stress of the core at the same depth. The possibility for hydraulic fracturing would be most critical when the reservoir rises to maximum pool quickly and the core does not have sufficient time to consolidate. (Kulhawy and Gurtowski, 1977)

5.3 Review of the Mindlin formulation

One of the fundamental results in the theory of elasticity is the Kelvin solution for a force applied at a point in a solid of indefinite extent. Such solution may be used in studying stresses due to a force applied at a great distance from a boundary. Another classical problem dealing with a

normal force applied at the plane boundary of a semi-infinite solid was solved by Boussinesq, and found practical application in the study of the distribution of foundation pressures, contact stress, and other problems in soil mechanics.

The solutions described by Mindlin (Mindlin, 1936) fill in the gap between Kelvin and Boussinesq solutions by giving the stresses for the case where the force is applied near the surface. Such a condition is approached in a number of practical problems including the case of a guy wire anchor, or by integrating these solutions along a line, we may approximate the conditions produced by a friction pile.

Mindlin solved two cases:

a) A force normal to the boundary of a semi-infinite solid.

b) A force parallel to the boundary of a semi-infinite solid.

In this study on hydraulic fracturing of clays the only case in which there is an application occurs when the force is normal to the boundary. This case will be presented here. For the solution of a force parallel to the boundary, refer to Mindlin's paper published in 1936.

5.3.1 Mindlin solution for a force normal to the boundary of a semi-infinite solid

The semi-infinite solid is considered to be bounded by the plane z=0, the positive z-axis penetrating into the body. A force P is applied at (0,0,c) and acts in the positive z direction. (Fig. 5.3) The boundary conditions are:

$$(\sigma_z)_{z=0} = (\tau_{rz})_{z=0} = 0 \qquad \text{Eq.5.1}$$

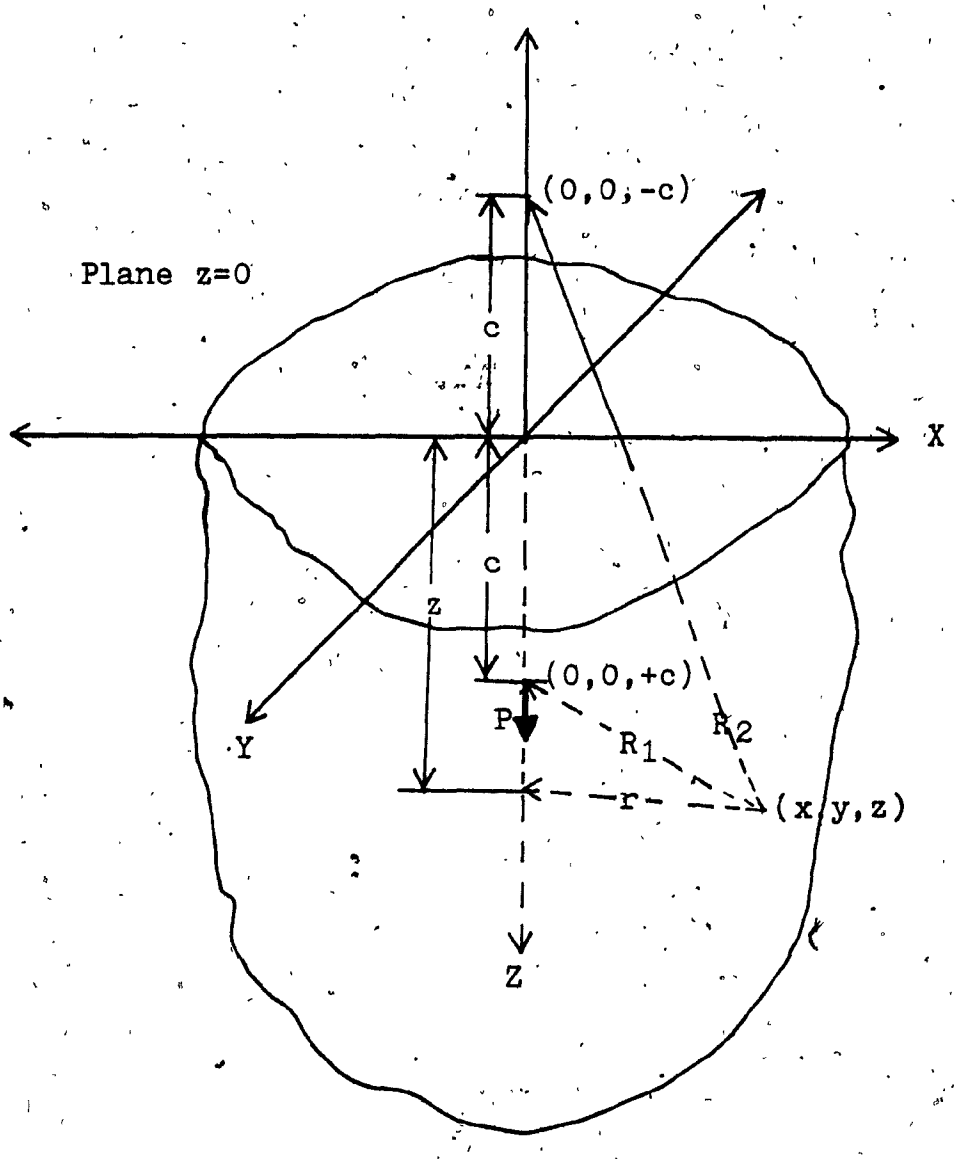

Fig. 5.3.
Force normal to the boundary in the interior of a semi-infinite solid

The equilibrium condition is:

$$P = -\int_0^L 2\pi r \sigma_z \, dr \,, \quad (z>c) \qquad \text{Eq. 5.2}$$

After some mathematical manipulations, the displacements and stresses are:

$$u = \frac{Pr}{16\pi G(1-\nu)} \left(\frac{z-c}{R_1^3} + \frac{(3-4\nu)(z-c)}{R_2^3} - \frac{4(1-\nu)(1-2\nu)}{R_2(R_2+z+c)} + \right.$$
$$\left. + \frac{6cz(z+c)}{R_2^5} \right) \qquad \text{Eq. 5.3}$$

$$w = \frac{P}{16\pi G(1-\nu)} \left(\frac{3-4\nu}{R_1} + \frac{8(1-\nu)^2 - (3-4\nu)}{R_2} + \frac{(z-c)^2}{R_1^3} + \right.$$
$$\left. + \frac{(3-4\nu)(z+c)^2 - 2cz}{R_2^3} + \frac{6cz(z+c)^2}{R_2^5} \right) \qquad \text{Eq. 5.4}$$

$$\sigma_r = \frac{P}{8\pi(1-\nu)} \left(\frac{(1-2\nu)(z-c)}{R_1^3} - \frac{(1-2\nu)(z+c)}{R_2^3} + \frac{4(1-\nu)(1-2\nu)}{R_2(R_2+z+c)} \right.$$
$$- \frac{3r^2(z-c)}{R_1^5} + \frac{6c(1-2\nu)(z+c)^2 - 6c^2(z+c) - 3(3-4\nu)r^2(z-c)}{R_2^5}$$
$$\left. - \frac{30cr^2z(z+c)}{R_2^7} \right) \qquad \text{Eq. 5.5}$$

$$\sigma_\theta = \frac{P(1-2\nu)}{8\pi(1-\nu)} \left(\frac{(z-c)}{R_1^3} + \frac{(3-4\nu)(z+c) - 6c}{R_2^3} - \frac{4(1-\nu)}{R_2(R_2+z+c)} + \right.$$
$$\left. + \frac{6c(z+c)^2}{R_2^5} - \frac{6c^2(z+c)}{(1-2\nu)R_2^5} \right) \qquad \text{Eq. 5.6}$$

$$\sigma_z \frac{P}{8\pi(1-\nu)} \left[\frac{-(1-2\nu)(z-c)}{R_1^3} + \frac{(1-2\nu)(z-c)}{R_2^3} - \frac{3(z-c)^3}{R_1^5} \right.$$
$$\left. - \frac{3(3-4\nu)z(z+c)^2 - 3c(z+c)(5z-c) - 30cz(z+c)^3}{R_2^5} \right] \qquad \text{Eq. 5.7}$$

$$\tau_{rz} = \frac{P\,r}{8\pi(1-\nu)}\left[-\frac{(1-2\nu)}{R_1^3}+\frac{1-2\nu}{R_2^3}-\frac{3(z-c)^2}{R_1^5}-\right.$$

$$\left.-\frac{3(3-4\nu)z(z+c)-3c(3z+c)}{R_2^5}-\frac{30cz(z+c)^2}{R_2^7}\right] \qquad \text{Eq. 5.8}$$

where:

G = modulus of rigidity

ν = Poisson's ratio

$R_1 = (r^2 + (z-c)^2)^{\frac{1}{2}}$

$R_2 = (r^2 + (z+c)^2)^{\frac{1}{2}}$

The basic assumptions are:

a) The solid is assumed to be isotropic, and homogeneous.

b) The solid is assumed to respond perfectly elastically to stresses.

5.4 Analysis of a special mode of instability of clays due to hydraulic fracturing

In 1981, Lefebvre, Philibert, Bozozuk, and Pare published a paper reporting experimentally a special mode of hydraulic fracturing of clays. They performed various hydraulic fracture tests in two soft clay deposits of different geologic origin and they found that the fracture mode was not unique. Instead, two distinct set of fractures developed; vertical fractures radiated out from the piezometer tips, and cracks inclined from 20 to 35 degrees from the horizontal formed an inverted cone-shaped fracture surface with its apex at the top of the piezometer.

The hypothesis that a unique fracture mode, that is, that only vertical fractures developed in normally consolidated clay, as Bjerrum, et al, (1972) reported, was not verified.

In the present thesis, a theoretical approach to the solution of hydraulic fracturing of over-consolidated clays is outlined. The analysis uses the Mindlin formulation, presented in the preceding section of this thesis, and the superposition principle.

The analysis shows that fracturing is the result of the hydraulic forces exceeding the tensile strength of the clay which are indirectly related to the in-situ stresses.

The mechanism of failure is assumed to be divided into two parts. (see Fig. 5.4)

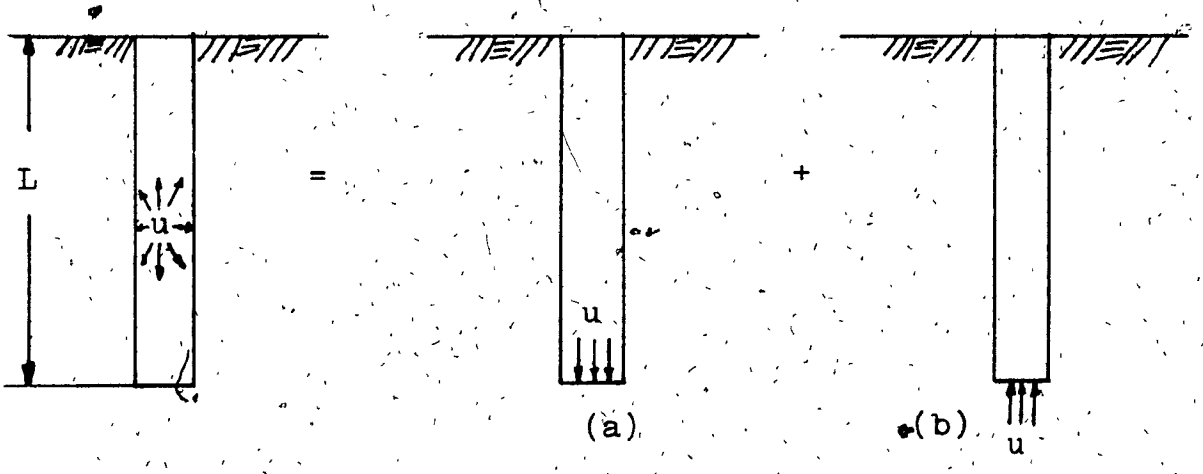

Fig. 5.4

Hydraulic Fracturing Failure Mechanism

From the ground surface to the tip of the piezometer, that is, case (b), the soil is assumed to behave as when a pile in clay is being pulled out; therefore, a solution for this type of problem is given, among others, by Poulus and Davis (1980).

Furthermore, from the tip of the piezometer to the interior of the clay, case (a), the soil is being compressed by the applied hydraulic pressure.

In this mode of failure, the change in length of the piezometer during the entire hydraulic fracturing test is constant since the piezometer is assumed to be rigid in comparison with the soil.

The following assumptions are made in the study of this mode of hydraulic fracturing of over-consolidated clays:

1) The soil is assumed to be isotropic, homogeneous, and of considerable extent compared with the dimensions of the piezometer.

2) The soil skeleton is assumed to be linear elastic. This assumption is justified since the clay is over-consolidated.

3) The piezometer is assumed to be rigid, and with a length great compared to the diameter.

With the assumptions given above, case (a) can be solved using the Mindlin formulation.

Therefore consider the case shown on Fig. 5.5

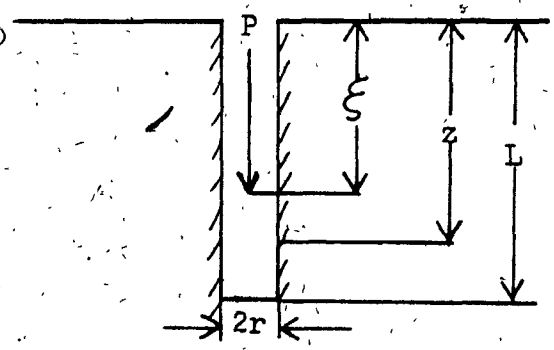

Fig. 5.5

Hydraulic Fracturing Problem

The Mindlin expression for the displacement in the z-direction is given by:

$$w(z) = \frac{P}{16\pi G(1-\nu)}\left[\frac{(z-\xi)^2}{R_1^3} + \frac{(3-4\nu)}{R_1} + \frac{5-12\nu+8\nu^2}{R_2} + \right.$$

$$+ \frac{(3-4\nu)(z+\xi)^2+2\xi(\xi+z)+2\xi^2}{R_2^3} + \qquad \text{Eq. 5.4}$$

$$\left. + \frac{6\xi z(z+\xi)^2}{R_2^5}\right]$$

where for isotropic materials $G = \frac{E}{2(1+\nu)}$

Let $I(\xi, z)$ be the influence value for a unit load at ξ causing movement w at z. That is, $I(\xi, z) = \frac{w(z)\,E}{P}$. Thus, equation 5.4 becomes:

$$I(\xi, z) = \frac{1+\nu}{8\pi(1-2\nu)}\left[\frac{(z-\xi)^2}{R_1^3} + \ldots\ldots + \frac{6\xi z(z+\xi)^2}{R_2^5}\right]$$

Eq. 5.9

Therefore, the total displacement in the z-direction due to the distributed load along the pipe axis is:

$$w_1(z) = \int_0^L \frac{P(\xi)\,d\xi}{E} I(\xi, z) \qquad \text{Eq. 5.10.a}$$

to which the component:

$$w_2(z) = \frac{\pi r^2 u I(L, z)}{E} \qquad \text{Eq. 5.10.b}$$

must be added.

Hence: $w(z) = w_1(z) + w_2(z)$

or, $$w(z) = \int_0^L \frac{P(\xi)\,d\xi}{E} I(\xi, z) + \frac{\pi r^2 u I(L, z)}{E} \qquad \text{Eq. 5.10.c}$$

Now, because any solution can be expressed in terms of a series expansion where the amount of terms depends on the

accuracy required, assume that the solution of $P(\xi)$ is given in the form: $P(\xi) = \sum_{n=0}^{\infty} b_n \xi^n$ Eq. 5.11

and substituting into Eq. 5.10.c we have:

$$w(z) = \frac{1}{E} \left(\sum b_n \xi^n I(\xi, z) \Delta\xi + \pi r^2 u I(L,z) \right) \quad \text{Eq. 5.12}$$

Therefore, the solution for the coefficients b_n, may be obtained from:

$$-\pi r^2 u I(L,z) = b_o(\sum I(\xi,z)\Delta\xi) + b_1(\sum \xi I(\xi,z)\Delta\xi) + \\ + \ldots + b_n(\sum \xi^n I(\xi,z)\Delta\xi) - E\, w(z) \quad \text{Eq. 5.13}$$

To ellaborate, consider (n+1) z points: 0, $z_1 = \frac{L}{n}$, $z_2 = \frac{2L}{n}, \ldots,$

$z_n = \frac{nL}{n}$.

Then, Eq. 5.13 reduces to:

$$b_o(\sum I(\xi,0)\Delta\xi) + b_1(\sum I(\xi,0)\xi\Delta\xi) + \ldots + b_m(\sum I(\xi,0)\xi^m\Delta\xi) + \\ \ldots - E\, w(0) = -\pi r^2 u I(L,0)$$

$$\vdots$$

$$b_o(\sum I(\xi,\tfrac{mL}{n})\Delta\xi) + b_1(\sum I(\xi,\tfrac{mL}{n})\xi\Delta\xi) + \ldots + b_m(\sum I(\xi,\tfrac{mL}{n})\xi^m\Delta\xi) + \\ \ldots - Ew(\tfrac{mL}{n}) = -\pi r^2 u I(L,\tfrac{mL}{n}) \quad \text{Eq. 5.14}$$

The influence value, I, can be known for a given Poisson's ratio, ν, which is a property of the material, and for a given position of the load P, ξ. Therefore,

$\sum I(\xi,z)\xi^n\Delta\xi$ is equal to a constant, c_{nz}.

Hence,

$$\begin{aligned} c_{oo}b_o + c_{o1}b_1 + \ldots\ldots - Ew(0) &= -\pi r^2 u I(L,0) \\ c_{1o}b_o + c_{11}b_1 + \ldots\ldots - Ew(1) &= -\pi r^2 u I(L,\tfrac{L}{n}) \\ \vdots \qquad \vdots \qquad\qquad \vdots \qquad\qquad &\vdots \\ c_{no}b_o + c_{n1}b_1 + \ldots\ldots - Ew(n) &= -\pi r^2 u I(L,L) \end{aligned} \quad \text{Eq. 5.15}$$

If the change of length, L is to remain constant during the hydraulic fracturing test, then:

$$w(0) = w(1) = w(n) = w \qquad \text{Eq. 5.16}$$

Therefore, the above set of (n+1) equations has (n+2) unknowns: b_o, b_1, ... , b_n; and w. One more equation is needed to obtain a unique set of values. This additional equation makes use of the condition of equilibrium, which is:

$$\int_0^L P(\xi)\, d\xi = 0 \quad \text{or,} \quad b_n \frac{L^{n+1}}{n+1} = 0 \qquad \text{Eq. 5.17}$$

Therefore,

$$c_{n+1,0} = \frac{L}{1}\ ; \quad c_{n+1,1} = \frac{L^2}{2}\ ; \quad c_{n+1,2} = \frac{L^3}{3}\ ; \text{ etc.}$$

and if $-\pi r^2 u I(L, \frac{mL}{n})$ is denoted as λ_m, then:

$$\begin{bmatrix} c_{oo} & c_{o1} & c_{o2} & \cdots & -E \\ c_{1o} & c_{11} & c_{12} & \cdots & -E \\ c_{2o} & c_{21} & c_{22} & \cdots & -E \\ \vdots & & & & \\ c_{n+1,o} & c_{n+1,1} & c_{n+1,2} & \cdots & 0 \end{bmatrix} \begin{bmatrix} b_o \\ b_1 \\ b_2 \\ \\ w \end{bmatrix} = \begin{bmatrix} \lambda_o \\ \lambda_1 \\ \lambda_2 \\ \\ \lambda_m \end{bmatrix} \qquad \text{Eq. 5.18}$$

The above procedure is valid only when the loading is rapid, otherwise, diffusion of water at the tip of the piezometer introduces another variable which cannot be easily accounted for.

The following computer program was developed to calculate the stresses in the soil due to case (a) of Fig. 5.4 only. The data required by the program is given below:

- Poisson's ratio for the soil,
- Modulus of elasticity for the soil, E, in psi.
- Length of piezometer or pipe, L, in inches.
- Radius of piezometer or pipe, r, in inches.
- Water pressure, in psi.

A sample calculation is given in Fig. 5.6, and the computer program is reproduced below.

```
]

?SYNTAX ERROR
]LIST.

100  PRINT "? POISSON'S RATIO"
101  INPUT MU
110  PRINT "? E OF SOIL"
111  INPUT E
120  PRINT "? PIPE LENGTH"
121  INPUT L
130  PRINT "? PIPE RADIUS"
131  INPUT A
140  PRINT "? WATER PRESSURE"
141  INPUT U
150  PRINT "NUMBER OF SEGMENTS REQUIRED"
151  INPUT NS
160 DX = L / NS
170  FOR I = 0 TO NS
180 X = I * DX
190 K1 = (1 + MU) / ((8 * E * 3.14) * (1 - MU))
200 K2 = (X - L) / (A ^ 2 + (X - L) ^ 2) ^ 1.5
210 K3 = (3 - 4 * MU) / (A ^ 2 + (X - L) ^ 2) ^ .5
220 K4 = (5 - 12 * MU + 8 * MU ^ 2) / (A ^ 2 + (X + L) ^ 2) ^ .5
230 K5 = ((3 - 4 * MU) * (X + L) ^ 2 - 2 * L * (L + X) + 2 * L ^ 2) / (A ^ 2 + (
X + L) ^ 2) ^ 1.5
240 K6 = 6 * X * L * (L + X) ^ 2 / (A ^ 2 + (X + L) ^ 2) ^ 2.5
250 B(I) =  - 3.14 * (A ^ 2) * U * K1 * (K2 + K3 + K4 + K5 + K6)
255  PRINT "X="X
260  NEXT I
270 I = NS + 1
280 B(I) = 0
290  FOR I = 0 TO NS + 1
300  PRINT "B("I")="B(I)
310  NEXT I
315  PRINT "."
316  PRINT "."
317  PRINT "."
318  PRINT "I'M CALCULATING.DON'T BUG ME"
400  FOR I = 0 TO NS
410 X = I * DX
420  FOR J = 0 TO NS
430 Z = J * DX
450 K2 = (X - Z) / (A ^ 2 + (X - Z) ^ 2) ^ 1.5
460 K3 = (3 - 4 * MU) / (A ^ 2 + (X - Z) ^ 2) ^ .5
470 K4 = (5 - 12 * MU + 8 * MU ^ 2) / (A ^ 2 + (X + Z) ^ 2) ^ .5
480 K5 = ((3 - 4 * MU) * (X + Z) ^ 2 - 2 * Z * (Z + X) + 2 * Z ^ 2) / (A ^ 2 + (
X + Z) ^ 2) ^ 1.5
490 K6 = 6 * X * Z * (Z + X) ^ 2 / (A ^ 2 + (X + Z) ^ 2) ^ 2.5
500 C(I,J) = K1 * (K2 + K3 + K4 + K5 + K6)
530  NEXT J
540  NEXT I
600  FOR I = 0 TO NS
610  FOR J = 0 TO NS
615 Z = 0
620 D(I,J) = C(I,J) * DX * Z ^ J
630 E(I,J) = E(I,J) + D(I,J)
631 A(I,J) = E(I,J)
635 Z = Z + DX
636  IF Z <  = L THEN  GOTO 620
650  NEXT J
```

```
660  REM A
670 J = NS + 1
680  FOR I = 0 TO NS
690 A(I,J) =  - 1
700  NEXT I
710 I = NS + 1
720  FOR J = 0 TO NS
730 A(I,J) = (L ^ (J + 1)) / (J + 1)
740  NEXT J
750  FOR I = 0 TO NS + 1
760  FOR J = 0 TO NS + 1
770  PRINT "A("I","J")="A(I,J)
780  NEXT J
790  NEXT I
791  PRINT "."
792  PRINT "."
793  PRINT "I'M CALCULATING.O.K?"
794  PRINT "."
800  FOR I = 0 TO NS + 1
810 A(I,NS + 2) = B(I)
820  NEXT I
830  FOR I = 0 TO NS + 1
840  FOR J = 0 TO NS + 2
850 Z(0,J) = A(0,J)
860 AN(I,J) = A(I,J) / A(I,I)
870  NEXT J
880  FOR P = I + 1 TO NS + 1
890  FOR J = I TO NS + 2
900 AN(P,J) = A(P,J) - AN(I,J) * A(P,I)
905 Z(P,J) = AN(P,J)
910  NEXT J
915  NEXT P
920  FOR S = I + 1 TO NS + 1
925  FOR T = I + 1 TO NS + 2
930 A(S,T) = AN(S,T)
935  NEXT T
940  NEXT S
945  NEXT I
950  FOR I = NS + 1 TO 0 STEP  - 1
955  FOR Q = NS + 1 TO I + 1 STEP  - 1
960 SUM(I) = SUM(I) + Z(I,Q) * X(Q)
965  NEXT Q
970  FOR R = NS + 1 TO 0 STEP  - 1
975 X(R) = (Z(R,NS + 2) - SUM(R)) / Z(R,R)
980  NEXT R
985  NEXT I
990  FOR I = NS + 1 TO 0 STEP  - 1
995  PRINT "ALFA("I")="X(I)
1000  NEXT I
1010 Y = 0
1015 SUM = 0
1020  FOR I = 0 TO NS
1030 BETA(I) = X(I) * Y ^ I
1040 SUM = SUM + BETA(I)
1050  NEXT I
1055 SS = SUM
1065  PRINT "Z="Y,"SIGMA="SS
1067 Y = Y + .1 * L
1070  IF Y <  = L THEN  GOTO 1015
```

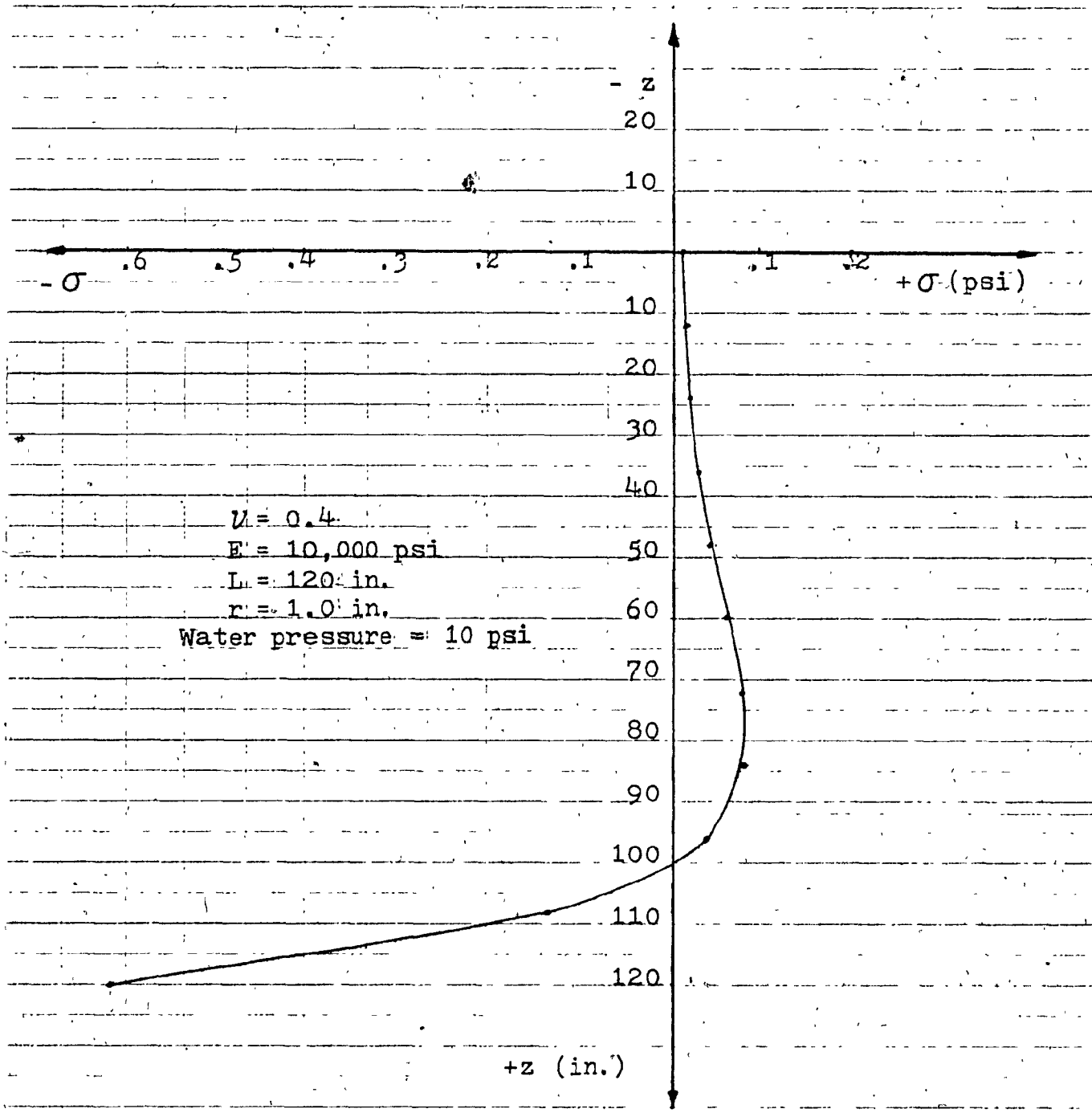

Fig. 5.6

Hydraulic Fracturing Results' Sample

CHAPTER 6

CONCLUSIONS

The main conclusions that can be drawn from this research study are as follows:

6.1 Analysis of the Flow of Liquefied Sand Deposits

The experimental and theoretical studies of the flow of liquefied sand deposits indicate that:

1. Mine Tailings, which have a wide variation of grain size distribution, tend to liquefy and flow over substantial distances posing a threat to life and property.
2. The flume experiments conducted as part of this research study indicate that the extent of the flow of liquefied sand is limited if the downstream slope is horizontal. However, the steeper the downstream slope, the more critical a failure would be.
3. The shape of the valley plays an important role in the extent of damage that a failure could cause.
4. The behaviour of liquefied sand deposits during flow is non-Newtonian and it can be best represented by the Bingham Plastic Rheological Model.
5. The perturbation technique for the analysis of laminar flow of liquefied tailings developed by Jeyapalan (1980) was found to be applicable.

6.2 Analysis of a Special Mode of Instability of Clays due to Hydraulic Fracturing

The study of the hydraulic fracturing of clays can be concluded as follows:

1. If the test is conducted in normally consolidated clays, then the problem is similar to the solution of a spherical cavity as given by Bishop, Hill, and Moot (1945).
2. If the clay is over-consolidated, then the hydraulic fracturing will be in the form of a tension zoned as observed in the laboratory experiments and as reported by Lefebvre, et. al. (1981).
3. The Mindlin formulation has an application in the theoretical analysis of the instability of over consolidated clays due to hydraulic fracturing.
4. The hydraulic fracturing is the result of the hydraulic forces exceeding the tensile strength of the clay which are indirectly related to the in-sity stresses.

6.3 Suggestions for Further Research

The following topics are considered suitable as an extension to the study described in this thesis:

1. The earthquake flume can be modified to study the flow failure of liquefied sand deposits in steeper slopes. This creates an extra-driving force that will require different analyses procedures.
2. Further research is needed to find a reliable way of

measuring the viscosity and the yield shear strength of liquefied sand. These two parameters are essential for the Bingham Plastic Model.

3. The study of the hydraulic fracturing of clays can be extended to the case where the loading is not rapid.

REFERENCES

1. Bishops, Hill, and Mott, "The Theory of Indentation and Hardness Test", Proceedings, Physical Society, Vol. 57, 1945.

2. Bjerrum, L., and Andersen, K.H., "In-situ Measurement of Lateral Pressures in Clay", Proceedings of the 5th. European Conference of the I.S.S.M.F.E., Vol. 1, Madrid, 1972.

3. Bjerrum, L., Nash, J.K.T.L., Kennard, R.N., and Gibson, R.E., "Hydraulic Fracturing in Field Permeability Testing", Géotechnique, Vol. 22, No.2, 1972.

4. Clark, J.B., "An Hydraulic Process for Increasing the Productivity of Wells", Trans. Am. Inst. Min. Eng., Vol. 186, January 1949.

5. Coates, D.F., and Yu, Y.S., Editors, Pit Slope Manual, Chapter 9, Waste Embankments, Ottawa, Canada, 1982.

6. Cramer, S.D., and Marchello, J.M., "Numerical Evaluation of Models Describing Non-Newtonian Behaviour", Trans. Am. Inst. Chem. Eng. J., Vol. 14, November 1968.

7. Dorby, R., and Alvarez, L., "Seismic Failures of Chilean Tailings Dams", Journal of the Soil Mechanics and Foundations Division, ASCE, November 1967.

8. Henderson, F.M., Open Channel Flow, The Macmillan Company, New York, 1966.

9. Hildebrand, F.B., Advanced Calculus for Applications, Prentice-Hall, Inc., Englewood Cliffs, New Jersey, 1962.

10. Hoare, B., "The Disposal of Mine Tailings Material", Ph.D. Thesis, University of Waterloo, Waterloo, Ontario, 1972.

11. Jaeger, J.C., and Cook, N.G.W., Fundamentals of Rock Mechanics, 3rd. edition, Chapman and Hall, London, 1979.

12. Jeyapalan, K., "Analysis of Flow Failures of Mine Tailings Impoundments", Ph.D. Thesis, University of California, Berkeley, August 1980.

13. Jeyapalan, K., Duncan, J., and Seed, H.B., "Summary of Research on Analyses of Flow Failings of Mine Tailings Impoundments", A Report Prepared for the U.S. Bureau of Mines Technology Transfer Conference, Spring 1981, in Denver, Colorado, December 1980.

14. Kulhawy, F., and Gurtowski,T., "Load Transfer and Hydraulic Fracturing in Zoned Dams", Journal of the Geotechnical Engineering Division, ASCE, Vol. 102, GT. 9, 1976.

15. Lefebvre, G., Philibert, A., Bozozuk, M., and Pare, J.J., "Fissuring from Hydraulic Fracture of Clay Soil", Proc. of the 10th International Conference on Soil Mechanics and Foundation Engineering, Stockholm, June 1981.

16. Mindlin, R.D., "Force at a Point in the Interior of a Semi-Infinite Solid", J. of Appl. Phys., Vol. 7, No. 5, 1936.

17. Mittal, H.K., "Design and Performance of Tailings Dams", Ph. D. Thesis, University of Alberta, Edmonton, Alberta, 1974.

18. Poulus, H.G., and Davis, E.H., Pile Foundation Analysis and Design, Wiley, New York, 1980.

19. Ritter, A., "Die Fortpflanzung der Wasserwellen", Zeitschrift des Vereines Deutscher Ingenieure, Vol.36, No. 33, 1892.

20. Schlichting, H., Boundary-Layer Theory. 7th edition, McGraw-Hill Book Company, New York, 1979.

21. Schowalter, W.R., Mechanics of Non-Newtonian Fluids, Pergamon Press, Oxford, G.B., 1978.

22. Westergaard, H.M., Theory of Elasticity and Plasticity, Dover Publications, Inc., New York, 1964.

23. White, F.M., Viscous Fluid Flow, McGraw-Hill Book Company, New York, 1974.

24. Williams, R.E., Waste Production and Disposal in Mining Milling and Metallurgical Industries, Miller Freeman Publications, Inc., U.S.A., 1975.